SLIDING CONTACT WEAR CAUSED BY LOOSE ABRASIVE PARTICLES IN INTERFACING LUBRICANT

By

ING-TSANN HONG

Bachelor of Science

National Central University

Chungli, Taiwan

1974

Submitted to the Faculty of the
Graduate College of the
Oklahoma State University
in partial fulfillment of
the requirements for
the Degree of
MASTER OF SCIENCE
December, 1980

SLIDING CONTACT WEAR CAUSED BY LOOSE ABRASIVE PARTICLES IN INTERFACING LUBRICANT

Thesis Approved:

Thesis Adviser

Dean of Graduate College

PREFACE

The purpose of this thesis is to investigate the phenomena of sliding contact wear caused by abrasive particles entrained in the interfacing fluid and to develop a Ferrographic-Wear model for predicting the related wear behaviour. This model was experimentally verified.

At this time, I would like to express my gratitude to my thesis adviser Dr. E. C. Fitch, Jr., for allowing me the opportunity to continue my graduate education. His guidance, encouragement, and inspiration have been an extremely valuable asset to me during my graduate work.

In addition, I would like to express my appreciation to my colleagues at the Fluid Power Research Center at Oklahoma State University for their assistance.

Most of all, I wish to extend my gratitude to my parents and wife for their support and understanding during my graduate endeavors at Oklahoma State University.

TABLE OF CONTENTS

LIST OF TABLES

LIST OF FIGURES

Figure

Page

Figure

Page

CHAPTER I

INTRODUCTION

It is commonly known that mechanical components can loose their usefulness in three major ways: corrosion, fatigue, and wear (1, 2). Essentially, wear is unavoidable. Friction exists whenever there is relative motion, and wear occurs due to friction. Thus, some wear at least is inevitable.

In the earlier period of the Industrial Revolution, the best that engineers could expect from their machines was that they would work at all. Today, it is much different story. Now, a machine is expected to not only function well, but also exhibit high efficiency, good reliability, and a long service life. Performance degradation and short working life in machines are usually caused by an almost trivial amount of material removed from critical surfaces due to wear. Energy crisis is now seriously felt everywhere, and "economic benefit" plays a major role in the field of machine design and maintenance. Consequently, the small amount of material worn, which was once considered trivial, is rapidly becoming important. Also, there will be a greater demand for longer life and higher reliability of equipment in the future. Thus, there are many

compelling reasons for gaining a better understanding of tribological wear and a better utilization of the results of wear research in engineering practice.

In general, machine components such as bearings, gears, and sliding mechanisms are devices which are both oil-wetted in service and sensitive to abrasive particles. In most applications, these components will be exposed to abrasive contaminants entrained in the lubricating medium. Rolling contact bearings are used to support rotating loads. The wear mechanism of rolling contact bearings is almost of a pure rolling type. The effect of abrasive particles on this mechanism has received much more attention compared to the other two types -- gears, and sliding mechanisms.

Research on ball bearing surface damage due to abrasive contaminant have been made (3, 4, 5, 6). Gears are usually found in a mechanical system and used to transfer power between two components. Damage due to wear in this component is always caused by the high pressure generated along the pressure angle where two teeth are forced to contact. Usually, this kind of wear is referred to as elastohydrodynamic (EHD) wear.

Although the study of wear on gears is very sophisticated due to the special mechanism involved, the EHD theory has been studied widely in tribology. Some investigators have documented the results of their research (2, 7). This will take the wear studies on gears out of the scope of the present study.

Sliding mechanisms are those mechanisms which have sliding relative motion, but do not have the primary function of a bearing or gear. Piston ring/cylinder, spool valve/housing assembly fall into this category. Contaminant induced wear between such sliding surfaces is of practical interest due to its widespread use. One would expect that much of the theoretical basis for its understanding would have been established for a long time. Actually, it is not true. Sliding mechanisms have received little or no attention with respect to abrasive contaminant wear in the interfacing fluid. The reported investigations of particle abrasive wear were usually restricted to dry-friction and utilized "two-body" abrasive models. The choice of the test specimens was at best peculiar (e.g., steel to diamond or to emery papers), and the results could not be easily applied by engineers in practical design situation related to lubrication and fluid power.

A thorough search of literature concerning the effects of abrasive particles on sliding contact wear revealed that methods used in tribological wear analysis were limited to the conventional intrusive techniques, dismantling the devices for making microscopic surface studies by the scanning electron microscope (SEM) or employing a "simulator" (i.e., attempt to relate the simulation results to the performance by duplicating some factors of interest). Actually, this technique is still classified as an intrusive method.

Generally, the components in sliding contact systems must be totally enclosed and it is virtually impossible to employ conventional wear analysis techniques to study the effected contaminant induced wear under realistic condition. Hence, a reliable and non-intrusive wear analysis method has been needed.

It has long been recognized that wear debris are a direct indicator of wear phenomena, especially in lubricated systems. Spectrographic debris analysis technique are now extensively used to analyze wear debris in lubrication oil but do not provide as much information as is desired (8, 9). For instance, this method can not distinguish between two samples containing foreign particles of very different average size but having the same total parts per million of contaminant. In addition to this drawback, spectrographs are sophisticated and expensive devices.

Ferrography (8, 9, 10, 11), is a new technique used to analyze wear debris from contaminated lubricant. It is capable of magnetically drawing wear debris from a lubricant onto a glass slide to yield a Ferrogram. Moreover the magnetic force arranges the debris almost according to their size on the slide. The density of the precipitating debris is determined by optical devices. This technique has been widely and successfully used for studying wear-related performance degradation in hyraulic and lubricating systems at the Fluid Power Research Center (FPRC), Oklahoma State University (OSU) since 1975. Fortunately,

in considering the wear of surfaces and mechanisms in hydraulic components as compared to those in lubricated components, a great deal of similarities exist. For example, a spool valve is similar to a sliding contact mechanism. Therefore, Ferrographic analysis techniques and the contaminant wear concepts developed at the FPRC to evaluate the phenomena of sliding contact wear due to abrasive particles in oils have been investigated for many years.

Because of the work mentioned above, this research effort was undertaken to investigate the wear associated with surfaces in contact where relative motion exists and various particle size distributions and concentrations of oil-entrained abrasives are exposed through Ferrographic wear analysis techniques.

A Ferrographic-Wear model is described for a contaminanted lubricant associated with a sliding contact mechanism, the model relates the wear rate of components to the amount of wear debris measured ferrographically. Besides developing and verifying the wear model, the phenomena of wear rate versus the clearence between two sliding surfaces is addressed and described in this report.

The remainder of this thesis presents and discusses the results of the total research program. The following chapters review previous related investigations in the area of abrasive wear and concepts associated with contaminated fluid wear. Chapter III presents the Ferrographic analysis

technique and develops Ferrographic-Wear models for predicting wear rate of sliding mechanisms under the influence of abrasive particles in lubricating fluids. Chapter IV delineates the experimental results of the Ferrographic-Wear model evaluation. Finally, Chapter V provides a summary and conclusions of the entire study. The Appendices contain some selected Ferrograms and the least squares curve fitting method for solving "log-log" problems.

CHAPTER II

RELATED INVESTIGATIONS

It was Leonardo da Vinci who found that wear increased with load and that the direction of wear is not necessarily in a vertical direction but follows the main vector of the load (12). Probably this description is a result of one of the systematic studies he made on wear phenomena.

Although wear behaviour has been studied for a long time, the fundamental principles are not yet well understood. There can be many reasons given for this poor progress but it is felt that the complexity of the wear mechanism itself may be the major reason. Even in recent years, of course, the formulation of an adequate and all embracing definition of wear is difficult. The American Society of Lubrication Engineering (ASLE) accepted the definition of wear as "removal of material by mechanical action" (13, P. 41), and a committee of the Institute of Mechanical Engineers defined it as "the progressive loss of substance from the surface of a body brought about by mechanical action" (14, P. 94). Both of these definitions are based on mechanical action and do not emphasise the causes due to chemical action. However, these definitions are acceptable as they are applied to the mechanism of

sliding wear caused by abrasive particles, since mechanical action predominates in such a process.

Wear, as previously noted, is not a simple process but involve complicated modes which can occur independently. In order to gain a better picture of this tribological phenomena, scientists have classified wear phenomena in a variety of ways. Most of them are based on the physical process, sliding process, or the results which are achieved (13). However, according to these classifications, at least four wear mechanisms can be summarized as follows:

1. Adhesive wear
2. Abrasive wear
3. Corrosive wear
4. Fatigue wear

In addition to these wear processes, Rabinowicz (15) added erosive wear and cavitation wear to enrich the classification. Erosive and cavitation wear normally occur between solid surfaces and the fluid. Sliding wear caused by abrasive particles, the subject studied in this research, falls into the categories of abrasive and erosive wear. Actually, erosive wear can be considered another form of abrasive wear (1), where wear rate is related to the kinetic energy of the particle. In most cased, erosion is a minor factor as compared to abrasion if they co-exist in the same system (1, 10, 14).

Abrasive wear usually occurs between two surfaces in

relative motion. The softer material will be plowed off due to the harder surface or hard particle between them. This wear covers two types of situations -- two-body abrasion and three-body abrasion, Figure 1. In two-body abrasive wear, a rough hard surface slides against a softer surface or hard embedded abrasive particles on one surface are directly in contact with the other softer surface. In three-body type, abrasion is caused by loose hard particles sliding between rubbing surfaces. Also, it occurs when clearances are small enough to trap abrasive particles between surfaces with enough force to result in the plowing or cutting action. Contamination wear falls into the category of embedded type or the three-body situation.

In an extensive search of the literature on abrasive wear and contaminant wear studies, it was found that most of the reported investigations recognized that wear is dependent on the properties of the abrasive particle, lubricant flow, component materials and other minor parameters like specimen size, and humidity. Therefore, it is felt that a brief review of these effects on abrasive wear would provide a strong background in developing a wear model in the next chapter.

Effects of Abrasive Particle Properties

Hardness, grain size and form, and grain concentration affect the wear behaviour caused by contaminant particles.

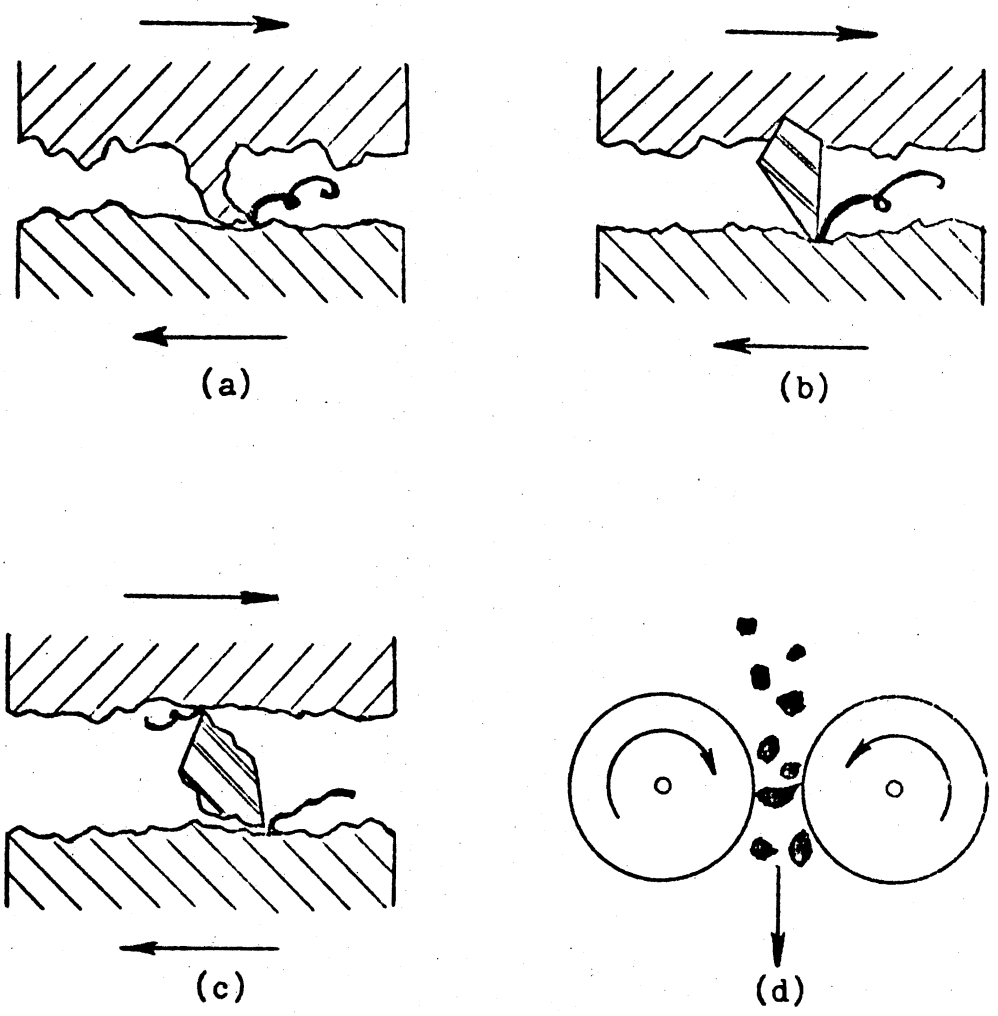

(a),(b): Two-Body Abrasion
(c),(d): Three-Body Abrasion

Figure 1. Mechanism of Abrasion

Several investigations (16, 17, 18) have shown that wear resistance depends on particle hardness.

Depending on the correlation between the hardness of abrasive particle, Ha, and the hardness of the metal, Hm, three distinct wear regimes can be observed as shown in Figure 2 (12). This characteristic has been confirmed by tests performed by both Wellingers and Stauff (19) and they stated that wear increases rapidly once the particle hardness exceeds that of the metal for both abrasive and erosive wear. Beyond this, the wear rate may become fairly constant or even reduce with increasing abrasive hardness. Moreover, Rabinowicz (20) reported that the wear resistance is approximately proportional to the hardness of the metal. this leads to the important conclusion that wear rate depends on the relative hardness of abrasive particles and test surfaces.

The particle grain size is a major factor affecting abrasive wear. Many of the references (17, 20, 21) state that the absolute wear rate increases with grain size up to some critical diameter, in general in the region from 50 micrometers to 80 micrometers, and then either slowly increases with grain size or remains constant. In order to confirm this behaviour, Sin (21) used test specimens sliding on different grades of SiC abrasive paper under a variety of load conditions. The results are depicted in Figure 3. This figure clearly show the effect of grain size on wear.

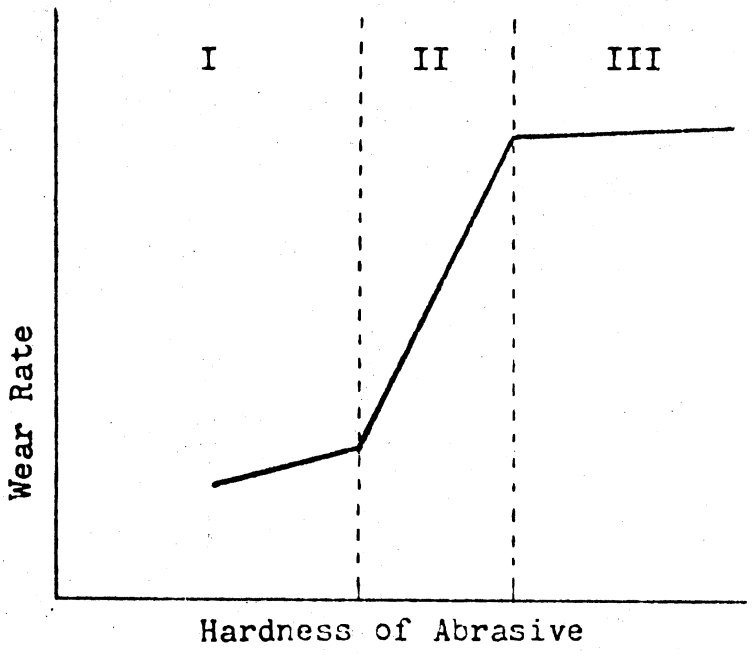

I: Low-Wear regime, if Ha < Hm
II: Transition regime, if Ha ≈ Hm
III: High-Wear regime, if Ha > Hm

Figure 2. Schematic of Effect of Abrasive Hardness on Wear Rate

Many tribologists attempted to find the reason why a constant wear rate results after some critical size is reached. Larsen Badse (23) postulates that this phenomena may be induced by specimen size since different lengths of an abrasive particles have different effect on the deterioration with different grit size.

Rabinowicz (24) suggested that the critical size effect is caused by the interference between adhesive and abrasive particles which is inversely proportional to the grain size. However, his research results were limited to qualitative description and experimental work only.

A quantitative expression was reported by Bergeron (19), from tests on Al.Br. He found that wear rate is proportional to (particle size)$^{0.75}$. Also, he stated that for general application, wear is proportional to the size times a function of coefficient of friction, densities, and size with surface curvature ratio. In addition to the effect of size on wear rate, particle shape also affects wear behaviour. The commonly accepted concept of this characteristics is that angular particles produce more wear than rounded particles (21).

Abrasive particles concentration is another factor that affects the wear rate, particularly in contaminant induced wear. Most contaminant-induced wear research was conducted by hydraulic engineers. It is generally accepted that wear increases with concentration (10, 25,

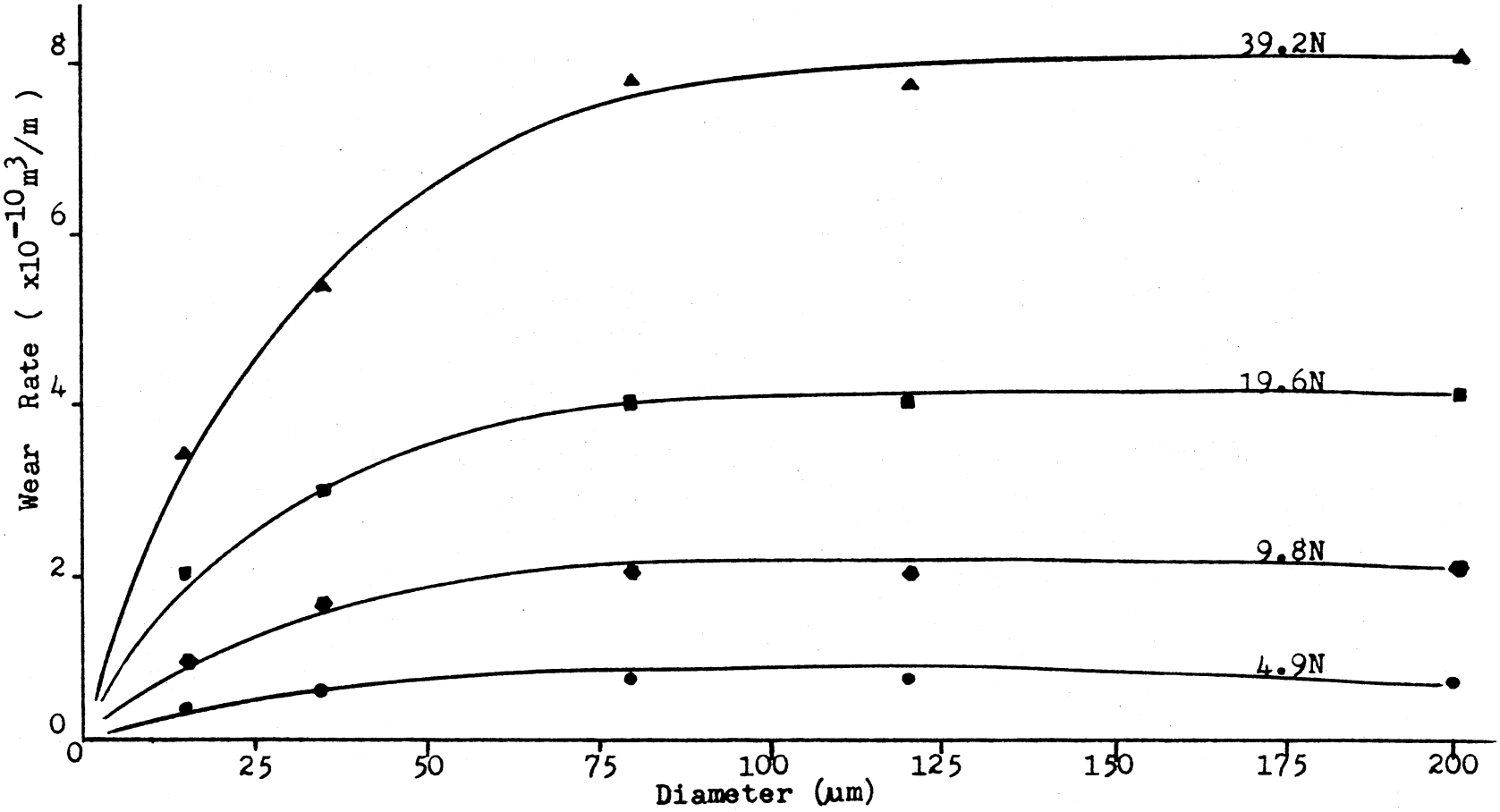

Figure 3. The Effect of Abrasive Grite Size on Wear Rate Under Different Normal Load

26, 27), and there exists a direct relationship between wear rate and concentration. Unfortunately, only little quantitative information has been reported regarding this aspect.

In his research on the abrasive effect on the centrifugal pump, Vasiliev (19) found that was associated with the conditions when the volume concentration of sand was directly proportional to $(\text{Concen.})^{0.82}$ and independent of materials or flow properties.

Recently, effects of contaminant-induced wear on hydraulic components have been studied at the FPRC. It was found that performance degradation of a wear sensive hydraulic component bears a linear relationship with abrasive concentration (25). Furthermore, a quantitative equation was obtained to predict the particle concentration effect of gear pump flow degradation, namely $\Delta Q = kC$ where ΔQ is total flow degradation, k is proportional constant which depends on pump characteristic and C is contaminant concentration.

Effects of Variables Other Than Abrasive Particle Properties

Properties of lubricant flow, material used and specimen size have been shown (16, 23) as detectable effects on abrasive wear. In addition, frictional heating and humidity can also affect wear rate. However, if

process conditions are well controlled, these two parameters will be overshadowed by other major properties (28).

Khrushchov and Babichev (29) tested a great variety of materials in the high wear regime, i.e., regime III in Figure 3, to determine the relevant material properties that govern the abrasive wear behaviour. The results revealed that the wear resistance, i.e., the reciprocal of wear volume, is directly proportional to their hardness. This linearity between wear resistance and material hardness was utilized by an abrasive wear model suggested by Rabinowicz.

Flow properties are usually considered when particle erosive type abrasion becomes dominant in the wear system. Occasionally, this property is discussed in the contaminant induced wear category. There are many mathematical expressions that relate wear rate with flow speed (30, 31). Since almost none of the tests were done under the same conditions, this quantitative expression, therefore, are not unique. However, a brief conclusion that can be made is that all of them used a power law to describ the relationship between the flow velocity and wear rate. The power index of speed varied from 1.4 to 3.0 depending on the test material used.

Specimen size effects have been comprehensively studied by Larsen Badse (23) and other triobologists. Larsen Badse utilized rectangular specimens of OFHC copper

to slide against virgin SiC abrasive paper. They determined that the wear rate after the specimens were slided a short (2.3 mm) and a long (9.0 mm) distance, that the influence of specimen length on wear might be as much as 30%. The effect is due to the sharpening of the contacting abrasive grains over the initial distances of contact and to blunting and deterioration of the grain when the contact occurs. The effect on wear rate is small when grit life is either much longer or shorter than specimen contact but may be appreciable when the two values are of the same order of magnitude. This discovery has been used to explain the knee point in the performance curve that results from wear rate with grain size as mentioned earlier.

Methods to Simulate A System Having Abrasive Sliding Wear

In order to gain a better understanding of wear behaviour, a great number of wear tests have been developed and used. There being a great range of available materials and the various wearing environments, it is virtually impossible to develop a "perfect" wear test method for all possible cases. However, a lot of wear test techniques have been successfully developed and comprehensively employed. Abrasive wear tests are described in a great number of published paper.

According to the lubricating condition between

sliding surfaces and the way in which abrasive particles are entrained, wear tests are classified as unlubricated (dry) or lubricated sliding mechanism with well-controlled contaminant added or with self-generated abrasive particle. Sliding wear due to abrasive particles in the fluid does not belong to the regime of dry sliding mechanism. Therefore, efforts made in this study will address the survey of tests which have been done in the field of contaminant induced wear in fluid wetted components.

Wear tests conducted with self-generated contaminant in lubrication system have been used quite extensively, like the four-ball technique (32, 33). It always costs a great deal of time to "generate" suitable wear debris for a wear study. Naturally this is a time consumming job. Furthermore, extremely high contact stresses are generated between surfaces under test. This way the wear mechanism shifts to an entirely different mode than expected.

In a recently developed accelerated-type contaminant exposure test technique, contaminants are added externally and according to the program preset, has a trend to replace the role which has been utilized by conventional techniques, e.g., four-ball test. The contaminant added depend on the system requirements. Usually, silica, metal chips or additives as required are acceptable. Though the choice of additive is optional, silica is the most

popular contaminant selected. The reasons may be the hardness of silica that higher than normal metals, and dirt in operating system fluids always came from the environment which contains silica as the major solid contaminant. These factors cause the simulated system to be more realistic. The most widely used silica is Air Clear Fine Test Dust (ACFTD) in which the particle size distribution is precisely controlled by General Moters (34).

Wear Debris Analysis Techniques

The properties and shapes of wear debris has been given a lot of attention which is applicable in wear analysis for all non-intrusive techniques. Recently, the study of wear debris recovered from wearing system has become of great importance to industry. Many conclusions may be reached by simple visual observation with or without optical aids. However, techniques such as filtration separation, magnetic separation, radio-active tracers and spectrometers are commonly found to be utilized by tribologists to achieve their goals on wear debris studies. Of course, these techniques have been successfully employed to analyze wear debris characteristic for many years -- at least 25 years.

Filtration separation has been applied to remove wear debris from lubricant by means of a porous membrane filter with a pore diameter of about 1 μm (35). Then, an equal

volume of solvent is passed through the filter and air-dried. After carbon coating, the debris deposited on the filter can be examined by the Scanning Electron Microscope (SEM).

Radioactive analysis methods were conducted by having radioactive treament on test parts prior to assembly. The degree of radioactivity in the fluid would provide an indication of the wear rate.

After evaluating both radioactive tracer and neutron activation methods, Tessman (10) suggested that neither of these two techniques are feasible for practical service due to their costly investment and sophisticated structure. In Chapter I, a comparison between spectrometer and magnetic seperation method (i.e., Ferrography) has been made. It was indicated that Ferrography has more benefit than the spectrometer. Likewise, as compared to filtration seperation methods, Ferrography is better since this method can separate wear debris from environmental type contaminant -- silica, while filtration technique can not. This implys that the most likely candidate for wear debris analysis is Ferrography.

Main Points Concluded From the Survey

An extensive literature search related to "sliding contact" wear caused by loose abrasive particles in fluids

was conducted. Owing to the large number of factors affecting wear behaviour in sliding contact mechanism, it was virtually impossible to identify an all-emcompassing relation for sliding contact wear. However, it is worth noting some general trends which were gained from the available literature for developing a Ferrographic-Wear model:

1. Wear increases with grain size up to a critical point then it remains constant or decreases slightly as grain size increases.
2. Wear rate also increases as contaminant concentration increases.
3. Wear depends on abrasive particle hardness, metal hardness, grain shape, specimen size, test environment, and frictional heating.
4. Wear increases rapidly with flow velocity which probably caused by erosive actions.
5. AC Fine Test Dust is a preferred contaminant for abrasive tests.
6. Ferrographic wear debris analysis technique has many benefits in lubricated wear studies as compared to other non-intrusive techniques.

CHAPTER III

FERROGRAPHY AND FERROGRAPHIC SLIDING WEAR MODELS

Ferrography

Ferrography is a relatively new technique developed to analyze wear debris recovered from oil-wetted components. The reason for its immediate success and becoming widely employed in wear analysis is due to its ability to separate metallic particles from extraneous entrained contaminants in lubrication fluids. Particle separation is accomplished by passing an oil sample through a chemically treated microscope slide which is positioned at an angle with respect to a magnet to generate a high gradient field. Metallic particles are attracted and captured by the magnetic field as they pass down the slide. After a specific amount of liquid has passed across the slide, a washing and fixing cycle removes the residual fluid and fixes the precipitated particles on the slide firmly, now, the slide is called a Ferrogram.

Theoretically speaking, magnetic field strength is very sensitive to distance, usually this strength is inversely proportional to the square of distance. Thus,

the angle of inclination between the slide and the magnet causes a magnetic gradient along the slide and allows the wear debris to be deposited along the entire fluid path on the Ferrogram. Moreover, the wear debris also arranges itself almost according to its size individually with larger particles precipitating first. Figure 4 illustrates a Ferrogram.

After the Ferrogram has been prepared, a Ferrogram Reader and a Bichromatic microscope are frequently employed to further examine the precipitated wear debris on the slide. The Ferrogram Reader, or the so called Desitometer, are operated by impinging a beam of light on the Ferrogram and electronically reading the amount of light reflected.

Physically, metal chips on the Ferrogram are opaque and reflect the light. The reflected bulk of light is collected and sensed on a photocell. Since the extraneous entrained contaminants like slica do not reflect light, the light density sensed by the photocell is an indicator of the amount of metal debris on the Ferrogram.

Figure 4 depicts the structure needed to prepared a Ferrogram and the basic principle of Ferrogram Reader. In addition to the quantity of wear debris, the gross particle size distribution is also of interest. This is accomplished by reading the "density" at different positions on the Ferrogram. These readings are often named as D54, D50, D30, and D10. D54 means the density of the collected

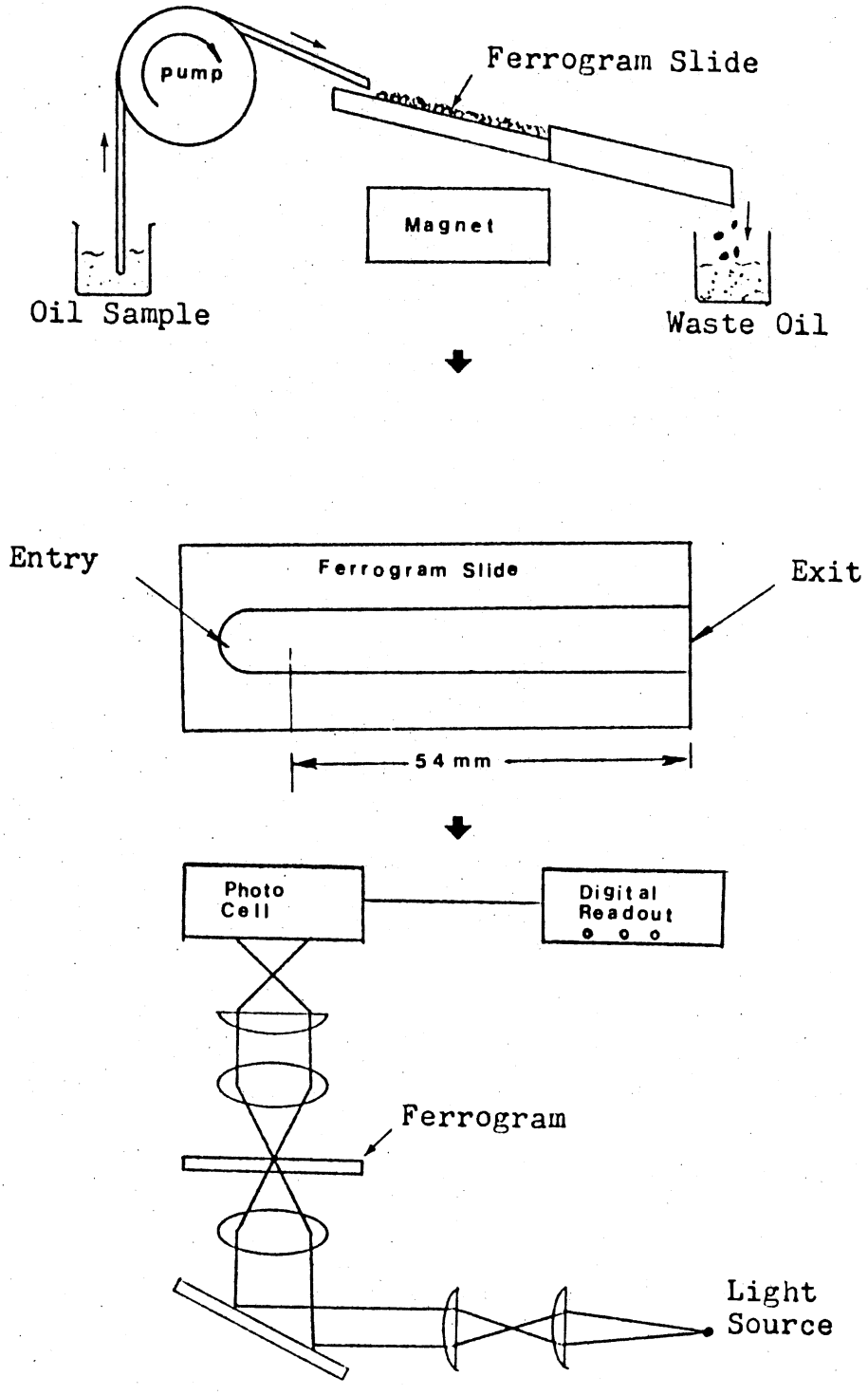

Figure 4. Illustration of Ferrography Devices and Ferrogram Slide

debris at a point which is 54 millimeters from the exit end. Likewise, the meaning of D50, D30, and D10 follows.

Generally, the high magnetic field gradient affects not only the size of wear debris collected but also the composition of particles. In fact, it is impossible to use Ferrograph Reader only to distinguish the free metal from compounds.

Fortunately, a device is available to overcome this problem, the Bichromatic microscope, Figure 5. Basically, the Bichromatic microscope has two light sources, one red and the other green. The red light is reflected from the specimen while the green light is transmitted through it. As previously stated, free metals are opaque and reflect red light. On the other hand, compounds reflect less or no light. Therefore, metals appear bright red and crystals appear highly green. The response of a compound depends on its composition. To distinguish them from each other is more of an art than a science.

The other instrument associated with Ferrography is called the Direct Reading Ferrography, or D.R.. This again is an optical density reader but does not need a ferrogram to be prepared. Instead of preparing a Ferrogram, a precipitating tube is used in a D.R. system for collecting wear debris by means of magnetic forces. Unlike the Ferrogram Reader, the D.R. measures the amount of light blocked by the particles present and converts

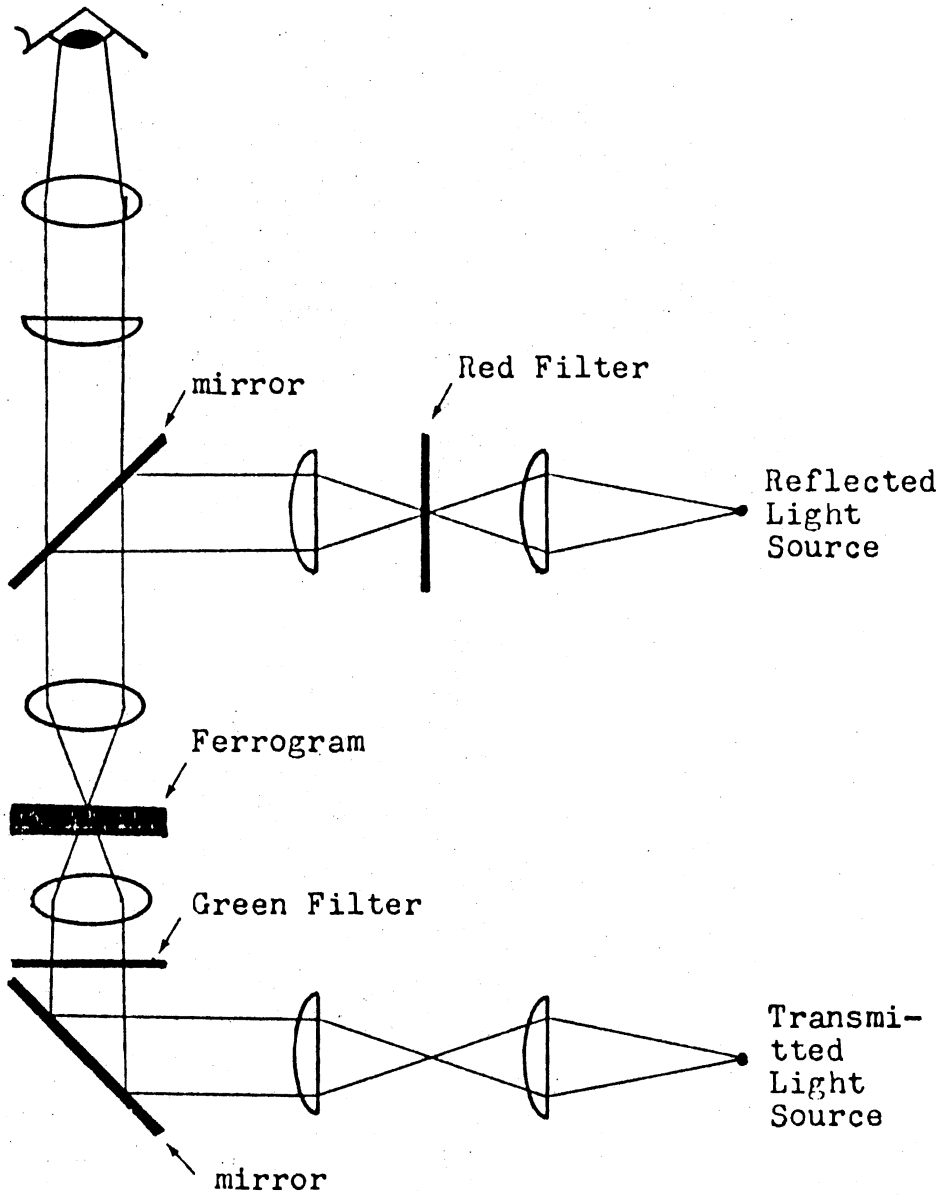

Figure 5. Schematic of Bichromatic Microscope

this to an optical density.

Evaluating Ferrographic Data

A ferrographic data is going to be used as the basis for formulating a ferrographic wear model for sliding contact, two key problems arise. Is ferrographic techniques reliable? What density reading from the Ferrogram Reader is the best one to fit the realistic condition? These two problems are very fundamental and very important.

In general, a reliable research analysis technique must meet three requirements: accuracy, repeatability and reproducibility. Certainly, no device can provide reliable analysis data unless the analysis results can be repeated within a small tolerance each time a given sample is analized. Moreover, if the results cannot be reproduced from one machine to another, it is difficult to generally accept them. In this regard, the Ferrography evaluation work done at the FPRC is invaluable.

Like any newly developed device, Ferrography faced a great number of problems in the earlier period (1974). At that time, the FPRC had expended a considerable effort to evaluate Ferrography. Fortunately, the results obtained from carefully and well-programmed experiments revealed that Ferrography is an acceptable technique in a wear analysis study. Experimental results (25) to demonstrate the repeatability and reproducibility are illustrated in

Figure 6. It is found that the maximum coefficient of variation exhibited by the data is about 5%.

Satisfactory Ferrogram data relating to the realistic wear behaviour depends on an adequate choice of the density reading. Dut to the complexity of wear processes, the choice of a "preferred" density reading from Ferrogram is quite unique in each case. However, Ferrography users should understand that, if some of the density readings are responsive to some type of test, it may be expected that they will be responsive to closely related tests. In order to find the best density reading to relate contaminant induced wear performance, a great number of correlation studies were carried out at the FPRC.

The test systems concerned were pump rotary mechanism and linear mechanism. The results revealed that the DRI, DEN, D54, and D50 readings are much more responsive to pump performance parameter changes than the DRE, D30, or D10 readings. DEN means the entry region density reading. DRI and DRE refer to the manufacture's designation of large and small values of DR respectively. Furthermore, the D54 readings follow equally well in the rotary and linear mechanism tests. Therefore, it is concluded that the particle density readings obtained at the 54 millimeters (D54) position on the slide is most responsive to wear mechanisms and is adopted in this research.

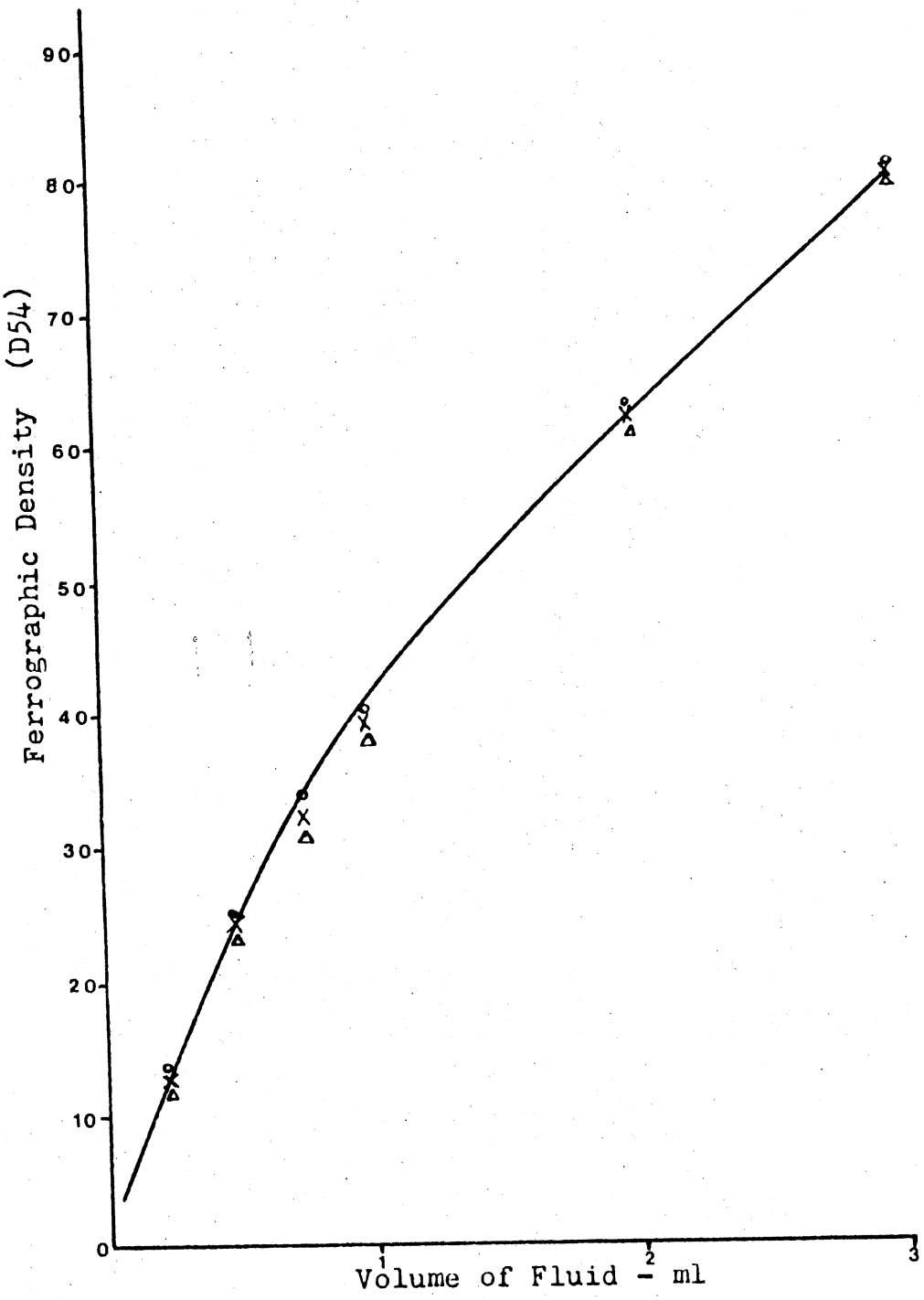

Figure 6. Repeatability and Saturation Characteristics of Ferrographic Techniques (25)

Mechanism of Sliding Contact Wear

In Chapter II, a comprehensive review of various abrasive mechanisms and data aquisition techniques was presented. This review provided a much clearer concept for developing a wear model concerning abrasive particles in interfacing fluids. However, in order to get a better understanding of the contaminant induced sliding contact wear mechanism, it is felt that a further study is needed.

It is a universal fact that wearing components have to go through three basic wear modes during their operating life, namely the break-in, normal, and the final failure modes. This process is illustrated in Figure 7 on a wear rate versus operating time curve. In the break-in wear mode, wear results from the presence of machined surface finishes, i.e., adhesive and two-body abrasion. It creates elongated free metal debris. The normal wear mode presents a gentle wear behaviour. The wear debris is not only small in size but also less in amount. Finally, when the component is approaching break down, the wear debris increases rapidly both in size and amount. Obviously, to accurately test a component's wear characteristics when exposed to an interfacing oil, the component should be in its normal wear mode.

Abrasive contaminant induced sliding wear can be defined as the wear associated with surfaces in contact where relative motion exits and abrasive particles which

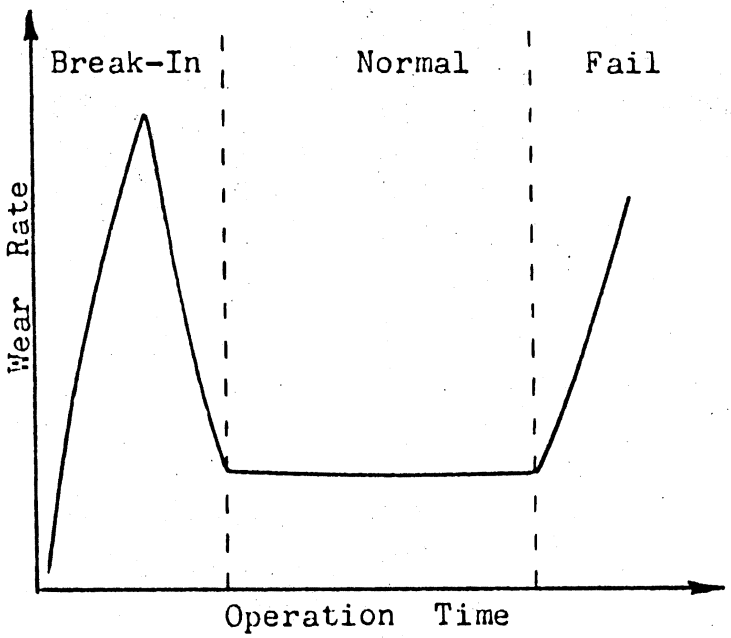

Figure 7. Components Wear Modes

are harder than the wearing surfaces are present. These extraneous entrained particles may cause abnormal wear in one of two ways (37), abrasive cutting wear or abnormal abrasive wear. The abrasive cutting wear occurs when one wearing surface is considerably harder than the other. The abrasive particles are embedded into the softer surface where they can act like a cutting tool to cut away the harder surface when sliding motion takes places between the contact surfaces. When the two wear surfaces are of comparable hardness, the abrasive particles roll between them and cause abrasive wear. Moreover, due to the repeated rolling, high local stresses on the contact surfaces may cause abnormal wear.

Contaminant Parameters

As previously noted, wear mechanisms are very complicated. The factors affecting wear behaviour are very sophisticated, too. Theoretically speaking, the wear rate should be a function of all the variables related to the wear processes of concern. It can be expressed as follows:

$$W = f(C,D,M,S,CM,HA,H1,H2,P,U,L,T,N,t) \qquad (1)$$

where: W = wear rate

C = particle concentration

D = particle size (distribution)

S = particle shape

CM = particle composition

M = particle mass

HA = particle hardness

H1 = wearing surface 1 hardness

H2 = wearing surface 2 hardness

P = load

U = lubrican flow speed

L = sliding distance

T = system temperature

N = effects by other minor factors

t = action time

Of course, it is impossible to analyze a wear system if consideration is not given to all the interacting factors. Usually, variables are kept constant except for those of special interest. Normally, there are four critical parameters which are of interest in contaminant-induced wear studies. They are particle size distribution, concentration, shape, and composition (10, 25, 36, 38). Furthermore, the abrasive particles chosen for contamination wear study are always pre-determined, e.g., ACFTD. Consequently, the properties of particle shape and composition are known in a given test. Therefore, Equation (1) can be simplified as follows:

$$W = f(D,C) \qquad (2)$$

Ferrographic Wear Model

Investigating component wear through the Ferrographic wear debris analysis technique is a newly developed method. Instead of representing wear rate in a conventional format, i.e., weight loss or dimension change, wear rate is expressed in terms of debris density reading on the Ferrogram. Problems encountered in developing a Ferrographic wear model related to some particular wear mechanism of interest would be as follows: (1) how to relate wear rate to Ferrographic density reading and (2) how to construct models to express wear rate with respect to particle size range and concentration in terms of density reading.

There is a considerable amount of work published on Ferrography. Most of the publish reports restrict themselves to instrumentation descriptions and operation theories which are basic and fundamental. And almost none of the investigators have paid much attention to the study of the relationship of Ferrography with the conventional technique. Therefore, major attention will be placed here on obtaining a relation to express Ferrographic density readings as a function of the wear rate.

As stated previously, Ferrography is a method to separate metal debris from the lubricant by means of magnetic force. Hence, the dynamic charateristics of

particles moving in a magnetic field determine the deposition charateristics of the debris.

In his report, "The Physics of Analytical Ferrography", Nair (39) derived a set of particle dynamic equations that govern particle behaviour in the formation of a Ferrogram. The equation set was developed for "ideal" conditions. The assumptions may be summarized as follows: the particles are evenly distributed in the fluid, the shape is spherical in nature, fluid flow properties are constant, and the ferrous particles in the sample do not interact with one another and do not combine together to form a layer of particles. Of course, such ideal Ferrography certainly does not exist in the realistic world; however, if the test was done in a well-controlled laboratory, this engineering idealization is reasonable. There are two equations which govern the particle deposition and the area covered by debris with respect to particle diameter. They are:

$$Z_p = \frac{A}{D_i^2} \left(\frac{Xoi}{h} - 0.25 \right) \qquad (3)$$

where: A = a constant of the Analytical Ferrogram for a given field and material of the particles.

D_i = the ith particle diameter.

Xoi = height location where the particle enters onto the slide.

Z_p = particle location.

h = maximum thickness of fluid film.

and

$$S_o = \frac{\pi^2}{16Ab'} \cdot \sum_{i=r}^{k} D_i^4 n_i \, (dZ_p) \qquad (4)$$

where: S_o = the area covered by the particles in the aperture of the optical densitometer.

b' = the width of the Ferrogram deposit measured laterally.

i = suffix, varies from r to k.

n_i = the number of particles of diameter D_i.

dZ_p = 0.1 cm corresponds to the aperture of the densitometer.

Figure 8 depicts the relationships of variables in Equation (3) and (4).

As previously stated, the Ferrogram density reader reads out the debris density according to the intensity of reflected light from the Ferrogram. Theoretically, the amount of reflected light is directly proportional to the area where light impinges on the Ferrogram. This area is the total debris surface exposed to the aperture of the optical densitometer, namely the term S_o in Equation (4). Thus, the density reading at some special position, for example D54, is proportional to the surface area S_o. It can be expressed as

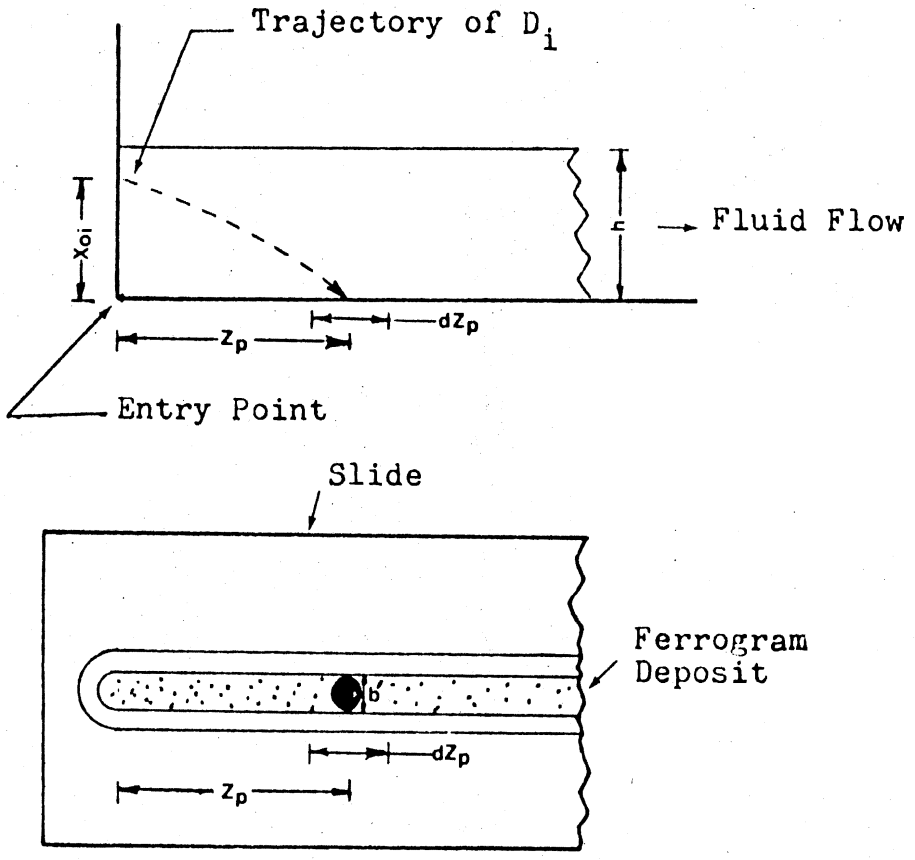

Figure 8. Illustration of Ferrogram Variables Relationships

$$FD(1) = k_1 S_o \tag{5}$$

where: $FD(1)$ = ferrogram density reading at 1 millimeters from the exit.

k_1 = proportionality constant.

Since the components have a constant wear rate during the normal wear mode, this indicates that n_i in Equation(4) can be treated as a constant at this moment. The term dZ_p as expressed in Equation (4) is always a constant. Thus, Equation (4) can be simplified to:

$$S_o = k_2 \sum_{i=r}^{k} D_i^4 \tag{6}$$

where: $k_2 = \pi^2 n_i(dZ_p)/16Ab$ is a constant in normal wear modes.

The weight or volume of wear particles is a direct indication of the severity and amount of wear. This implies that a weight loss or dimension decrease in the wear system results in the studying particle dynamic properties, the shape of wear particles is considered spherical in dealing with wear behaviour. Therefore, the weight of a wear particle with diamter D_i is:

$$w_i = \pi d D_i^3/6 \tag{7}$$

where: w_i = the weight of the ith wear particle.

d = density of the particle

or $$w_i = k_3 D_i^3 \tag{8}$$

where: $k_3 = d\,\pi/6$ is a constant if the debris composition is the same.

By relating Equations (5) and (6), it is found that the Ferrographic density reading at position 1 has a fourth power relation with particle size D_i, i.e.,

$$FD(1) = k_2 \sum_{i=r}^{k} D_i^4 \tag{9}$$

Combining Equations (8) and (9), we have

$$FD(1) = k_4 \sum_{i=r}^{k} w_i D_i \tag{10}$$

where: $k_4 = k_2/k_3$ is a constant.

Equation (3) implies that if the density readings are taken at a fixed position, e.g., l = 54mm, then the particle diameter D_i is constant in terms of Xoi. This characteristic is based on the fundamental principle of electromagnetics. Since Xoi has a numerical initial value, D_i again has a numerical initial value proportional to X_{oi}. This indicates that Equation (10) can be reduced to

$$FD(1) = k_5 \cdot \sum_{i=r}^{k} w_i \tag{11}$$

where: k_5 = a constant which depends on D_i.

The total wear as determined from the debris in fluids is the total sum of w_i. Therefore, the Ferrographic density reading is proportional to the total wear rates W

or $$FD(1) = k_5 W \tag{12}$$

Equation (12) states that the density reading at a "fixed" position is proportional to the realistic wear loss. Now, if a function relating both the contaminant particle size range and the particle concentration is known, then the Ferrographic wear model can be developed with the help of Equation (12).

From the published research results on the effect of grain size on abrasive wear by Sin (21), and others (20), it can be concluded that the wear rate increases with grain size till some critical size is reached, e.g., 80 micrometers, then the rate remains constant or slightly decreases as the grain size increases, as shown in Figure 3. However, a less quantitative expression relating wear rate and particle size has been found. Fortunately, the wear-size characteristics curve can be linearlized if the data are depicted in a log-log scale coordinate, as shown in Figure 9. Furthermore, the research efforts on contaminant induced wear on hydraulic component performance expended at the FPRC also reveals a log-log relation of degradation to contaminant size range, Figure 10.

Since hydraulic component performance degradation definately depends on the increased clearance due to wear (10, 25), the degradation curve in Figure 10 implies that wear is a log-log function of particle size. Therefore, it can be concluded that the role of sliding contact wear caused by abrasive particles entrained in the interfacing fluid would be a log-log function of particle size range. Thus, at a constant contamination level, this can properly be expressed as:

$$\log W = \log a + b \log D_u \tag{13}$$

or

$$W = a D_u^b \tag{14}$$

where: W = wear rate

D_u = particle size, upper limit of ACFTD cut.

a, b = constant parameters depends on system tested.

Equation (13) and (14) are applicable to predict the sliding wear behaviour in interfacing fluids except in the case of the "wedge" condition. Normally, wedging action occurs when the critical particles have sizes close to the dimension of the clearance between the wearing surfaces. From the work done in the valve contaminant sensitivity area, the force required to actuate the spool is a function of the particle size distribution of extraneous entrained contaminant (40).

The fact that wedging action exists in sliding

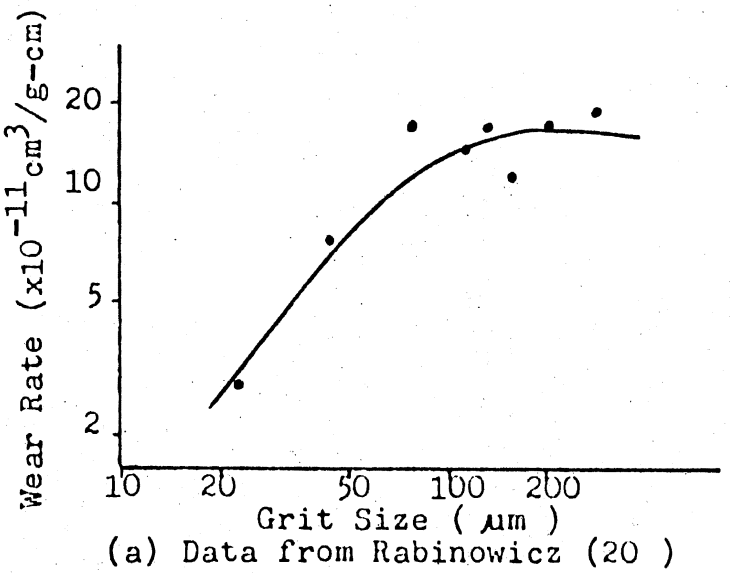

(a) Data from Rabinowicz (20)

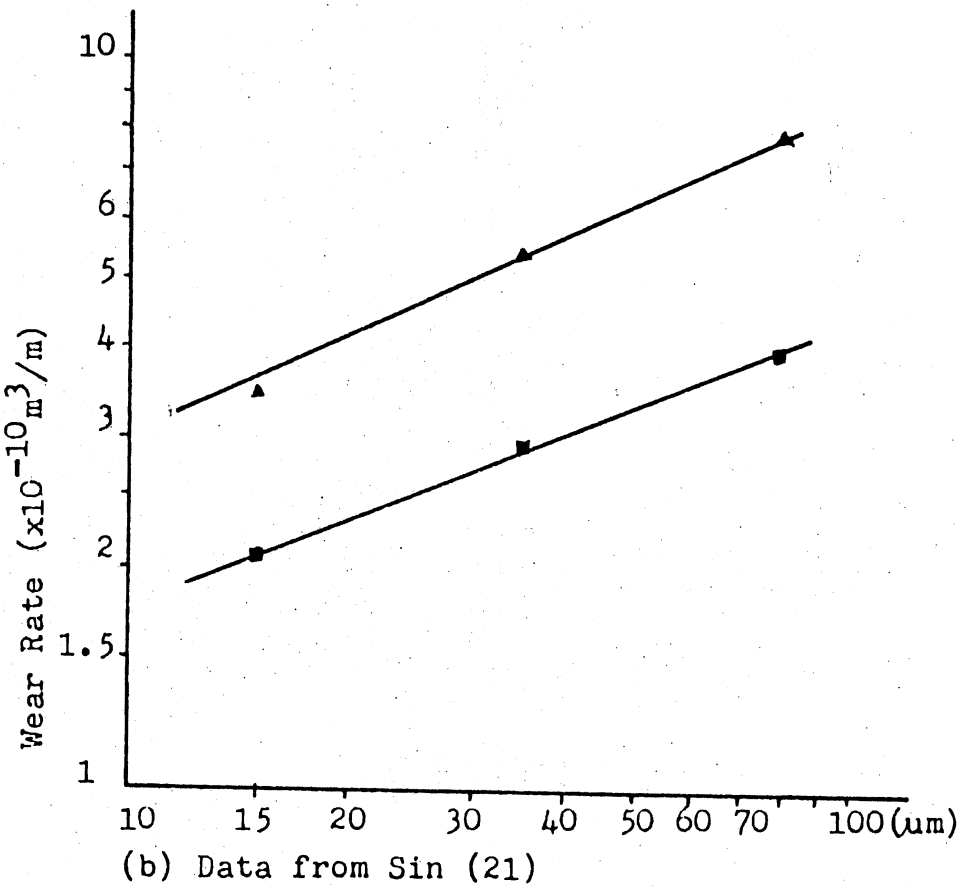

(b) Data from Sin (21)

Figure 9. Grit Size vs Wear Rate in Log-Log Scale

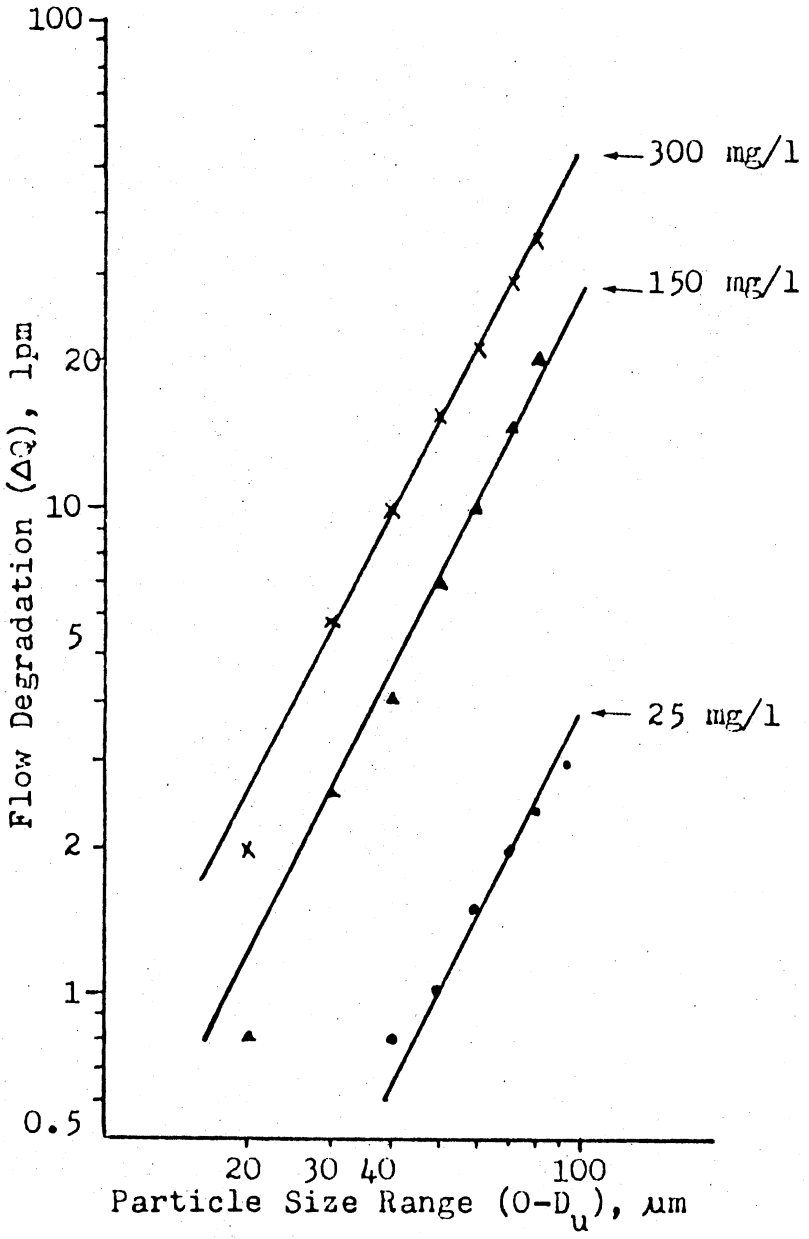

Figure 10. Pump Flow Degradation vs Particle Size

contact wear mechanism is not surprising. Usually, abrasion is more significant in the wedging condition and much wear debris generation can be expected. Figure 11 depicts the basic wedging mechanism postulated. Moreover, experimental data obtained from a spool valve test are shown in Figure 12 which confirms the principle postulated in this study.

Particle concentration also affects the fluid wetted component wear behaviour. From previous work on concentration studies, just as particle size is related to wear rate, particle concentration again has a log-log normal relationship with wear rate as shown in Figure 13, and expressed as:

$$\log W = \log c + d \log C \tag{15}$$

or

$$W = c\, C^{d} \tag{16}$$

where: W = total wear rate

C = particle concentration

c, d = constants which depends on testing condition

The similar influence of particle size range and concentration on wear rate is easy to understand since the increase in concentration causes an increase in the amount of abrasive particles. Unlike wear-particle size equations, however, wear concentration equations, i.e., Equation (14) and (15), are valid for all conditions

(a) Particle Size ≐ Clearance Space

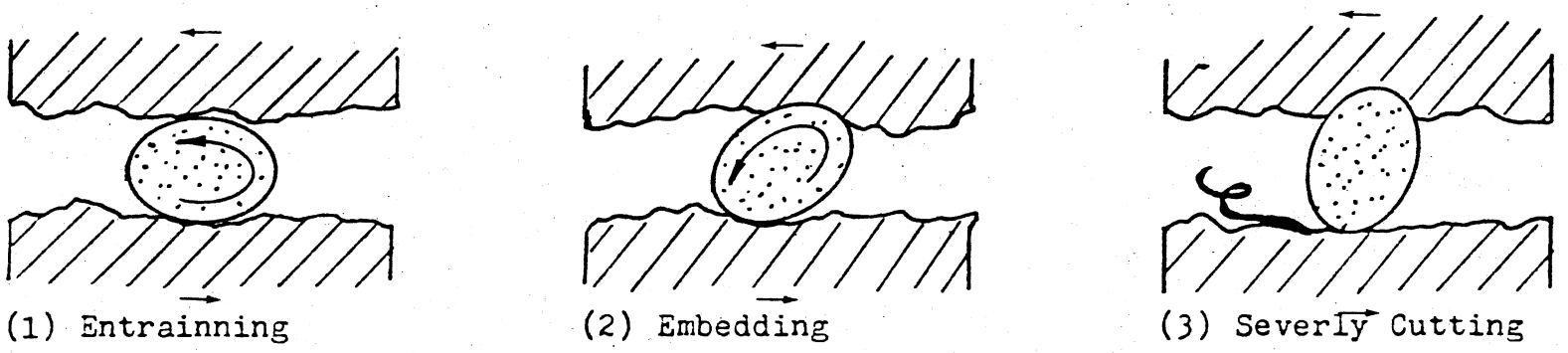

(b) Particle Size > Clearance Space

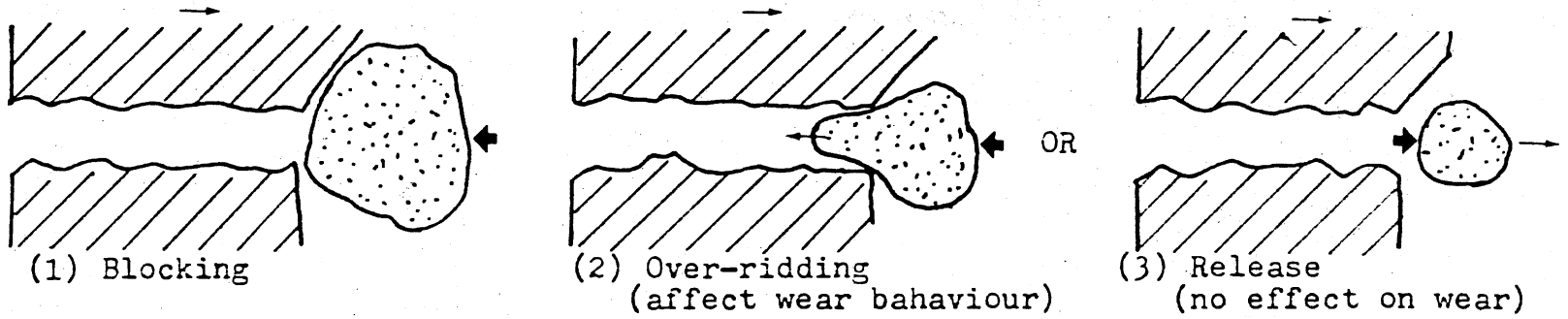

Figure 11. Mechanism of Wedge Phenomenon

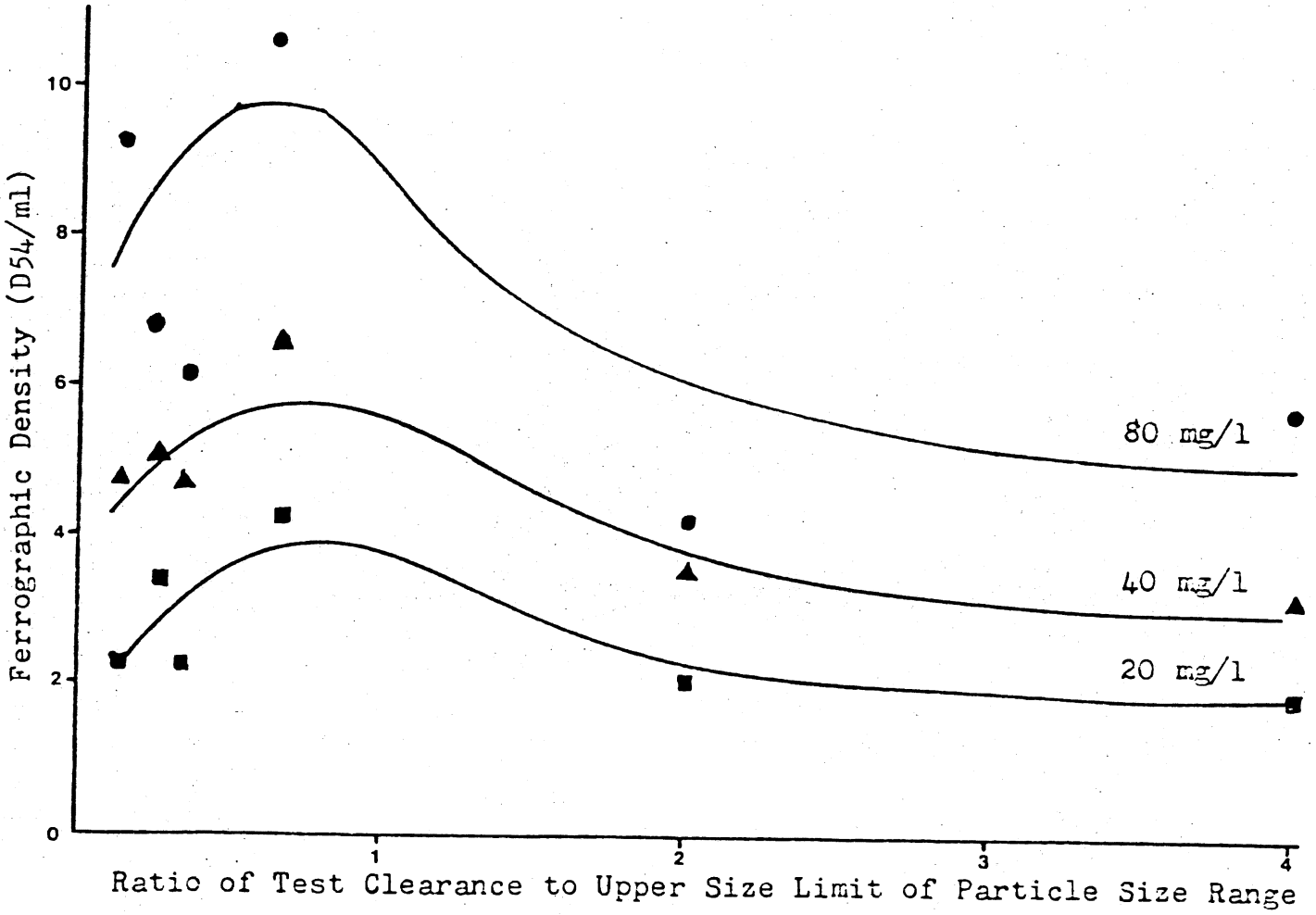

Figure 12. Contaminant Size and Concentration Effect at Various Clearance on Sliding Mechanism

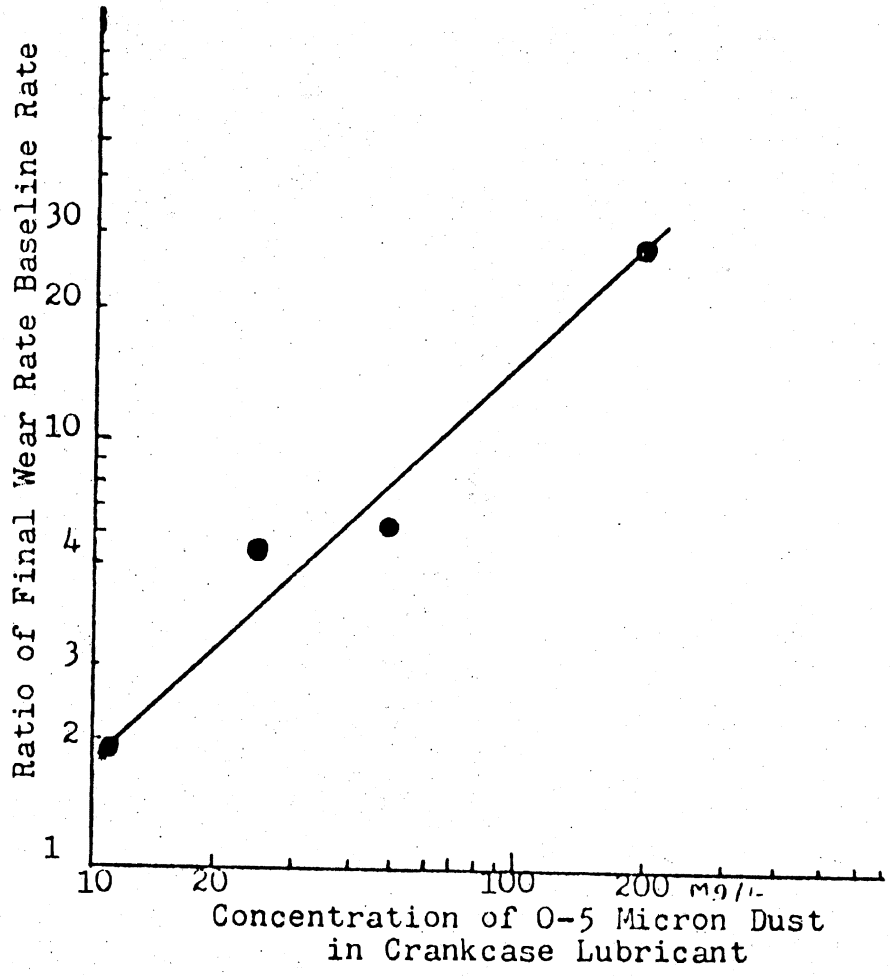

Figure 13. Particle Concentration Effect on Piston Ring Wear Rate (38)

including wedging action.

Finally, Equation (14) and (16) can be substituted into Equation (12) to yield the unique Ferrographic-Wear models. These models express the degree of contaminant induced sliding contact wear with respect to Ferrographic density reading, particle size range, D_u, and particle concentration C. As discussed previously, density reading at the 54mm position from slide exit, namely D54, is more responsive to wear behaviour; therefore, the Ferrographic-Wear models can be expressed as follows:

$$FD(54) = k_6 D_u^b \tag{17}$$

and

$$FD(54) = k_7 C^d \tag{18}$$

where: FD(54) = ferrogram density reading D54

k_6 = constant of coefficient, equals to $k_5 a$

k_7 = constant of coefficient, equals to $k_5 c$

In conclusion, the Ferrographic-Wear models developed in this study are applicable to abrasive particles induced sliding contact wear mechanisms except Equation (17) which will fail when applied to a wedging situation.

In order to verify the models that have been developed, tests have been conducted. These tests have already been completed by researchers at the FPRC during 1975-1977. The primary purpose of the tests was to study the

degradation of hydraulic components when they were exposed to contaminated lubricants. Fortunately, they were typical wear mechanisms of sliding contact caused by abrasive particles in interfacing fluids. A review of the test procedures and test results used to evaluate Ferrographic-Wear models are presented in the following chapter.

CHAPTER IV

EXPERIMENTAL VERIFICATION

Sliding contact mechanisms are usually found in a piston-bore combination of a piston pump or a spool valve. Normally, these wearing components are contained in a closed system thus it renders a direct investigation on component wear phenomena most difficult. The Ferrographic Wear model developed in Chapter III would provide an efficient way to overcome the problem mentioned.

It is felt that an experimental verification of those models is necessary before the model can be applied in the real world. During 1975 to 1977, two series of tests (36, 41) were performed at the FPRC to evaluate the performance degradation of hydraulic components. The linear mechanism in these tests were typical sliding type mechanisms. The tests are discussed here in order to evaluate the Ferrographic-Wear model. The models concerning the particle size range, concentration and wedge effect are verified with experimental data. A brief description of the test device and test procedures are presented here to convey a much clearer picture of the tests.

The devices used in both sets of tests are illustrated in Figure 14. These devices were designed to simulate

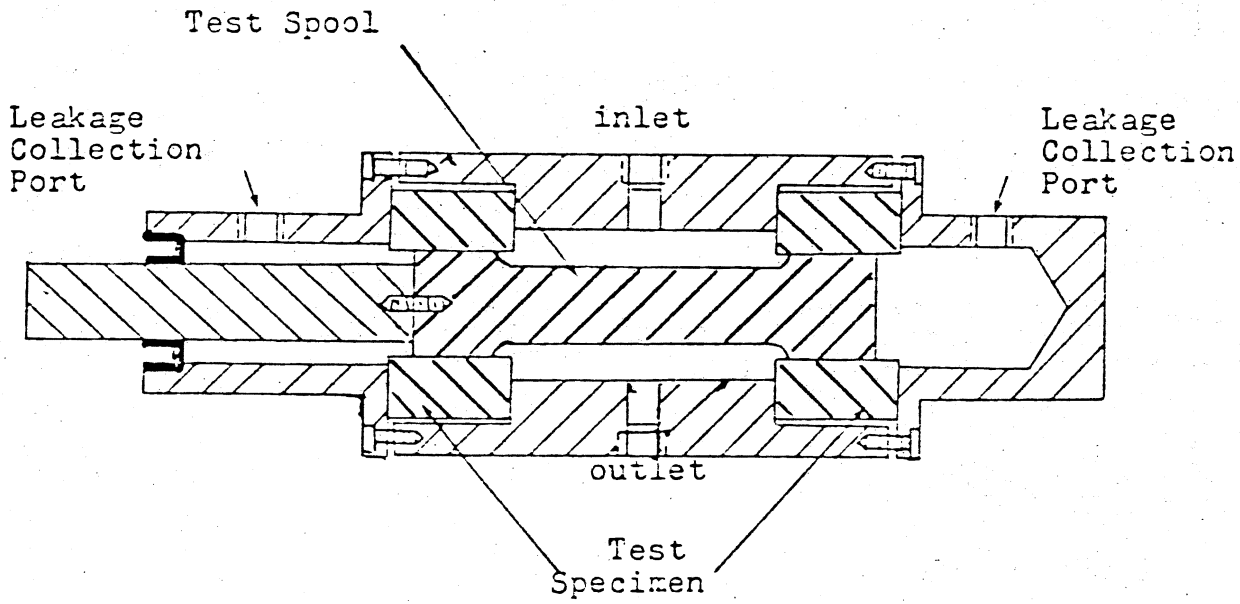

Figure 14. Schematic of Test Component

sliding contact wear mechanism. As shown, contaminated fluid enters the central chamber at test pressure. Two outlet ports were placed 90° from the inlets. The symmetry of the interior chamber provided a force balance at all chamber pressures. Upon entering the device the fluid divides into a flow stream through the outlets and a leakage flow between the spool and the bore. Leakage flow is plumbed back to the main return lines at a point down stream of the pressure drop valve located on the main return line just part the mechanism outlet. The leakage lines have valves to direct their combined flow to a sample tube.

The test specimen consisted of 1020 mild steel double-ended spool and two cast iron bore blocks. Bore diameters were nominally 12.70 millimeters and spool ends were lapped to match the situation required; for example, to a size of about 10 micrometers less than the bore diameter. A matched set of three pieces each was utilized for one particle size range of test dust with different concentration. Such a test system with a drive mechanism is shown in Figure 15.

Test Procedure

As previously stated, the studies on wear behaviour are preferred to be performed during the normal wearing mode as shown in Figure 7. Therefore, the components

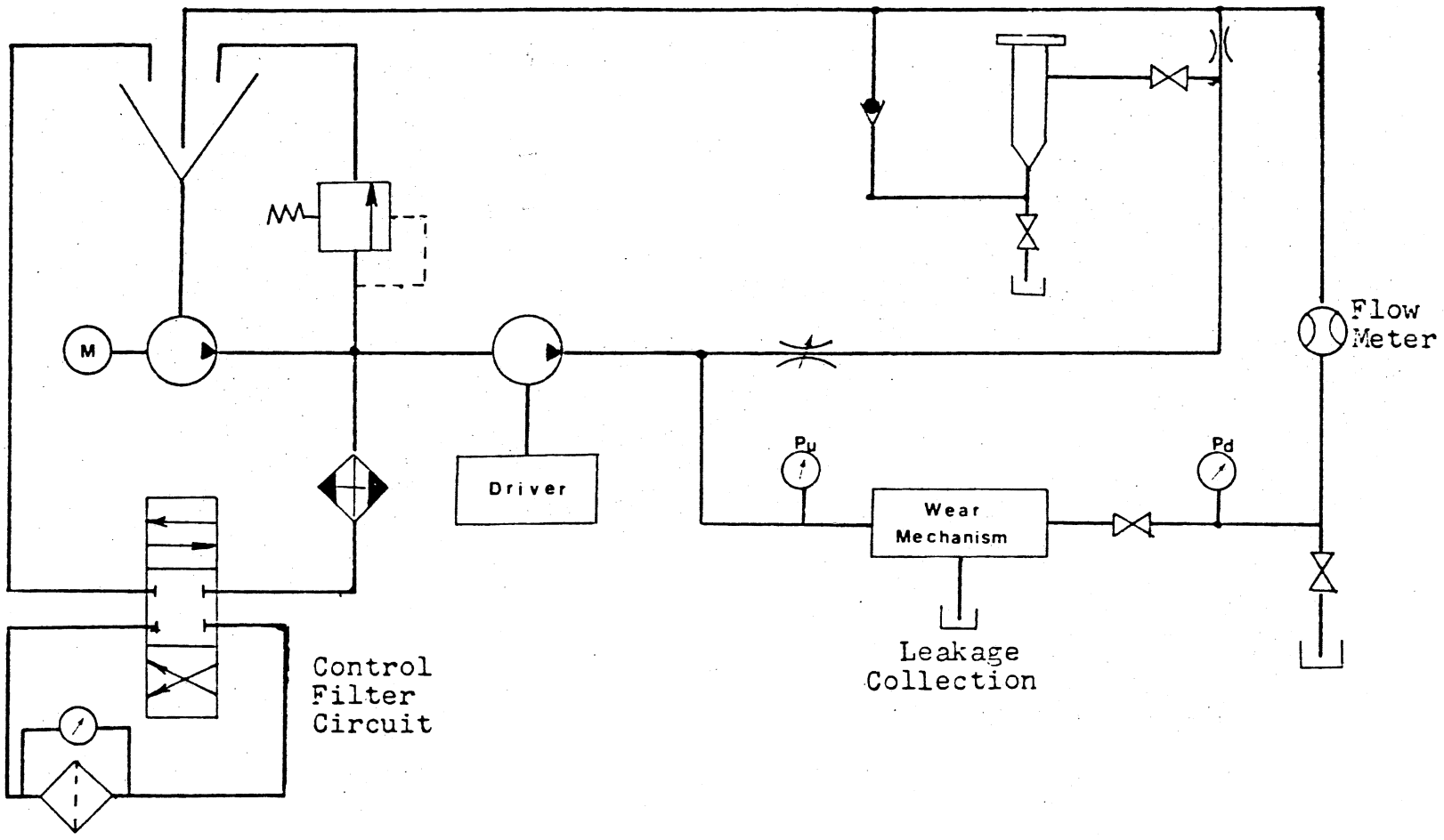

Figure 15. Schematic of Test System

have to undergo a break-in test. This test not only provides good wear test conditions but also checks the drive mechanisms for proper operation. The suggested break-in procedure is presented in Appendix A.

In order to focus on the wear phenomena related to particle size and concentration, the parameters listed below were held constant throughout the tests.

Pressure drop across test clearance	1,000	psi
Cycle rate of Mechanism	85	cpm
Fluid temperature	120	F
Total flow rate through the mechanism	3	gpm
Lubrication oil	MIL-5606	

The test specimens were numbered as 1-1, 1-2, 1-3, and 2-1, 2-2, 2-3. Specimens 1-1, 1-2, 1-3 underwent a normal wear test while specimens 2-1, 2-2, 2-3 underwent a wedge wear test. The test plan which was followed is illustrated in Table I. The test procedure was as follows:

1. Install specimens and conduct break-in test.
2. Establish test flow, pressure, and temperature with filters in the system and active mechanism.
3. Remove filters from flow loop.
4. Inject 5 milligrams per liter of 0-5 micrometre test dust classified from ACFTD.
5. Circulate oil with contaminant for 14 minutes taking sample at 2, 4, 8, and 14 minutes.

TABLE I

TEST PLAN

Specimen Number	Material	ParticleSize (μm)	Clearance (μm)	Contaminant Concentration (mg/l)
1-1	Cast Iron	0- 5	10	5,10,20,40,80
1-2	Cast Iron	0-30	10	5,10,20,40,80
1-3	Cast Iron	0-80	10	5,10,20,40,80
2-1	Cast Iron	0- 5	30	5,10,20,40,80
2-2	Cast Iron	0-30	30	5,10,20,40,80
2-3	Cast Iron	0-80	30	5,10,20,40,80

6. Filter circulating oil for 30 minutes.
7. Repeat steps 3-6 for concentration of 10, 20, 40, and 80 milligram per litre of 0-5 micrometre dust.
8. Repeat steps 1 through 7 for 0-30 and 0-80 micrometre contaminants.

Steps 1 through 8 are applied for testing specimens 1-1, 1-2, and 1-3. For testing specimens 2-1, 2-2, and 2-3, step 5 and step 6 were replaced by the following:

5. Circulate oil with contaminant for 45 minutes taking sample at 2, 7, 14, 25, and 45 minutes.
6. Filter circulating oil for 45 minutes.

Test Results

The data used in the wear rate evaluation for the sliding contact mechanisms tested were the density readings obtained from the Ferrographic oil analysis of the lubricant samples. The readings used in this study were the D54 values. During each injection in both the particle size test and concentration tests, four or five fluid samples were extracted. A D54 was obtained by normalizing the readings for a unit volume of fluid, e.g., 1 ml, and averaged them arithmatically to produce a mean D54 per millilitre per injection to be used in the wear rate evaluation.

The experimental results are listed in Table II, and the characteristic curves of D54 versus concentration and

TABLE II

TEST RESULT

Specimen Number	Particle Size(μm)	Concentration mg/l				
		5	10	20	40	80
1-1	0- 5	0.40	1.27	1.90	3.30	4.13
1-2	0-30	0.25	1.50	2.25	4.50	6.13
1-3	0-80	1.25	1.00	2.20	4.95	9.25
2-1	0- 5	2.50	1.20	1.98	3.14	5.70
2-2	0-30	2.12	2.71	4.01	6.60	10.75
2-3	0-80	3.48	2.22	2.63	4.64	6.70

D54 versus particle size range are illustrated in Figure 16, 17, and 18. Also the related Ferrograms are presented in Appendix C.

Verification of Ferrographic Wear Model

As developed in Chapter III, the Ferrographic-Wear models reveal that the Ferrographic density reading D54 has a log-log relationship to both particle size and concentrations. In other words, D54 is a power function in terms of size and concentration respectively. To accurately evaluate the properties of the Ferrographic-Wear models, experimental results were treated statistically. A set of equations was obtained by means of the least square curve fitting method. The modified least square method which can reduce the power equations to linear form are presented in Appendix B.

Table II lists the equation sets derived from the test results. The related coefficient of determination are also included. As can be seen from Table III, the experimental data agrees closely with the theoretically derived equation.

It is felt that the comparison shown in Figures 16-21 adequately demonstrates that the model can be applied to predicate wear rate precisely by the non-intrusive Ferrographic oil analysis technique.

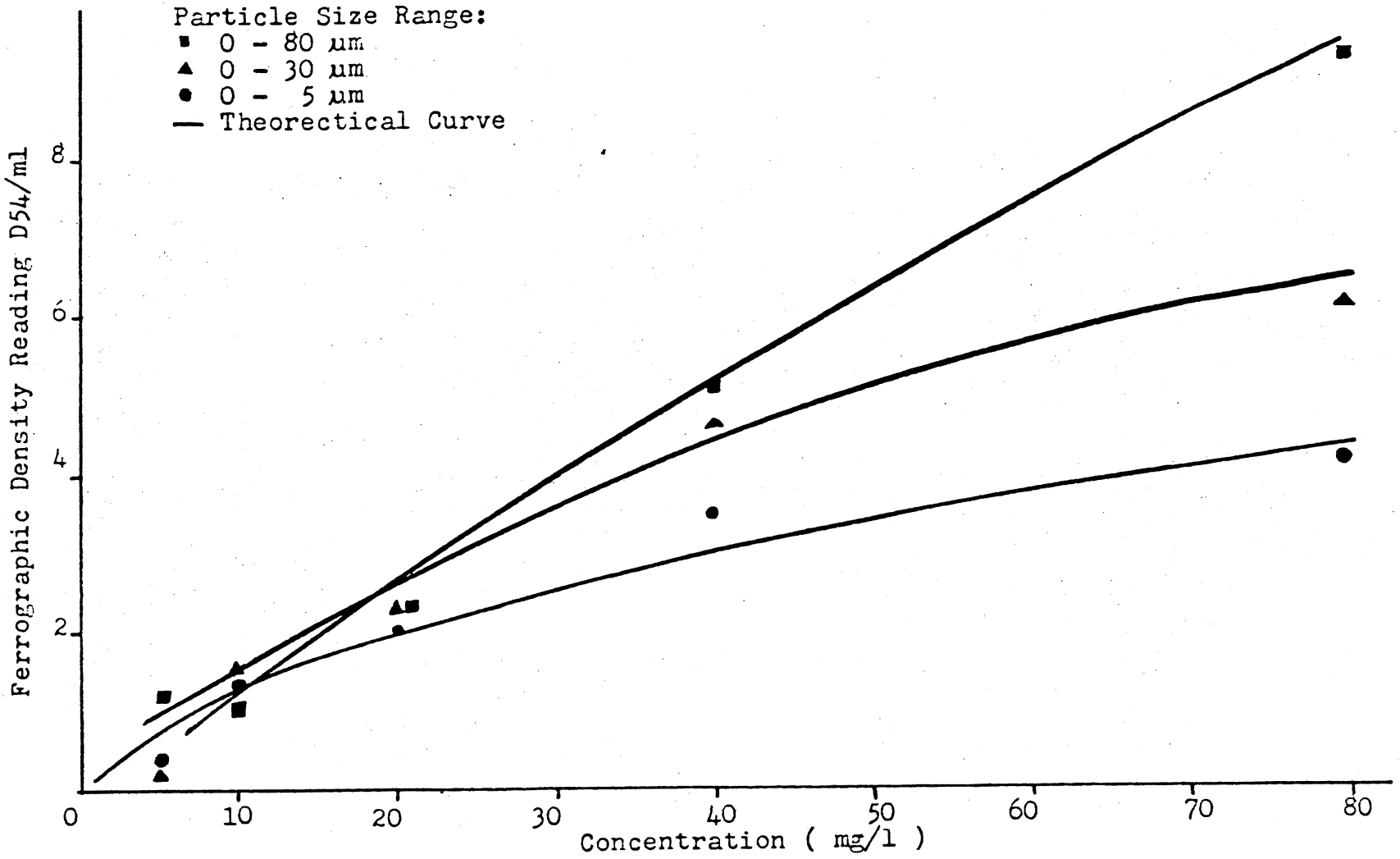

Figure 16. D54/ml vs Particle Concentration at Normal Condition

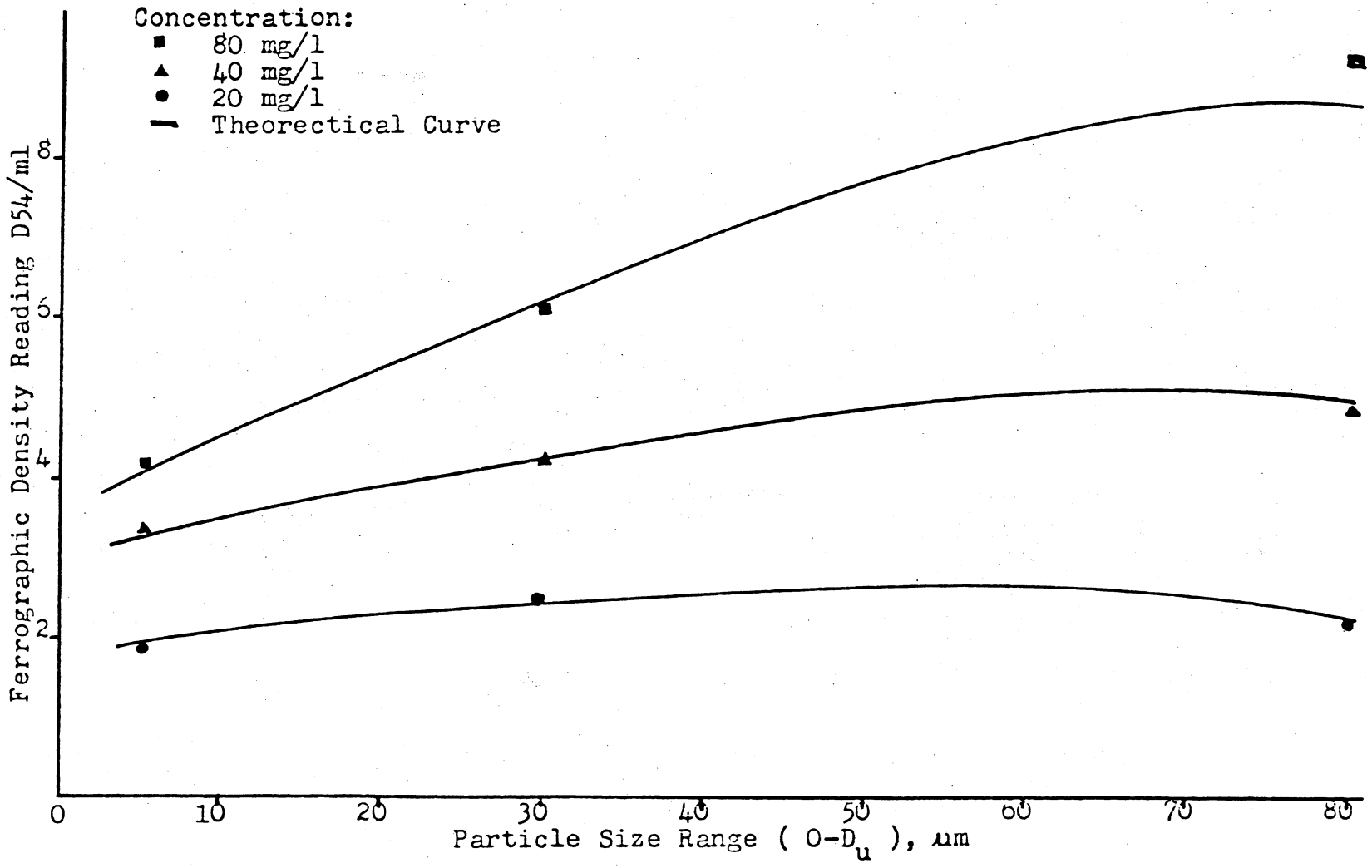

Figure 17. D54/ml vs Particle Size Range at Normal Condition

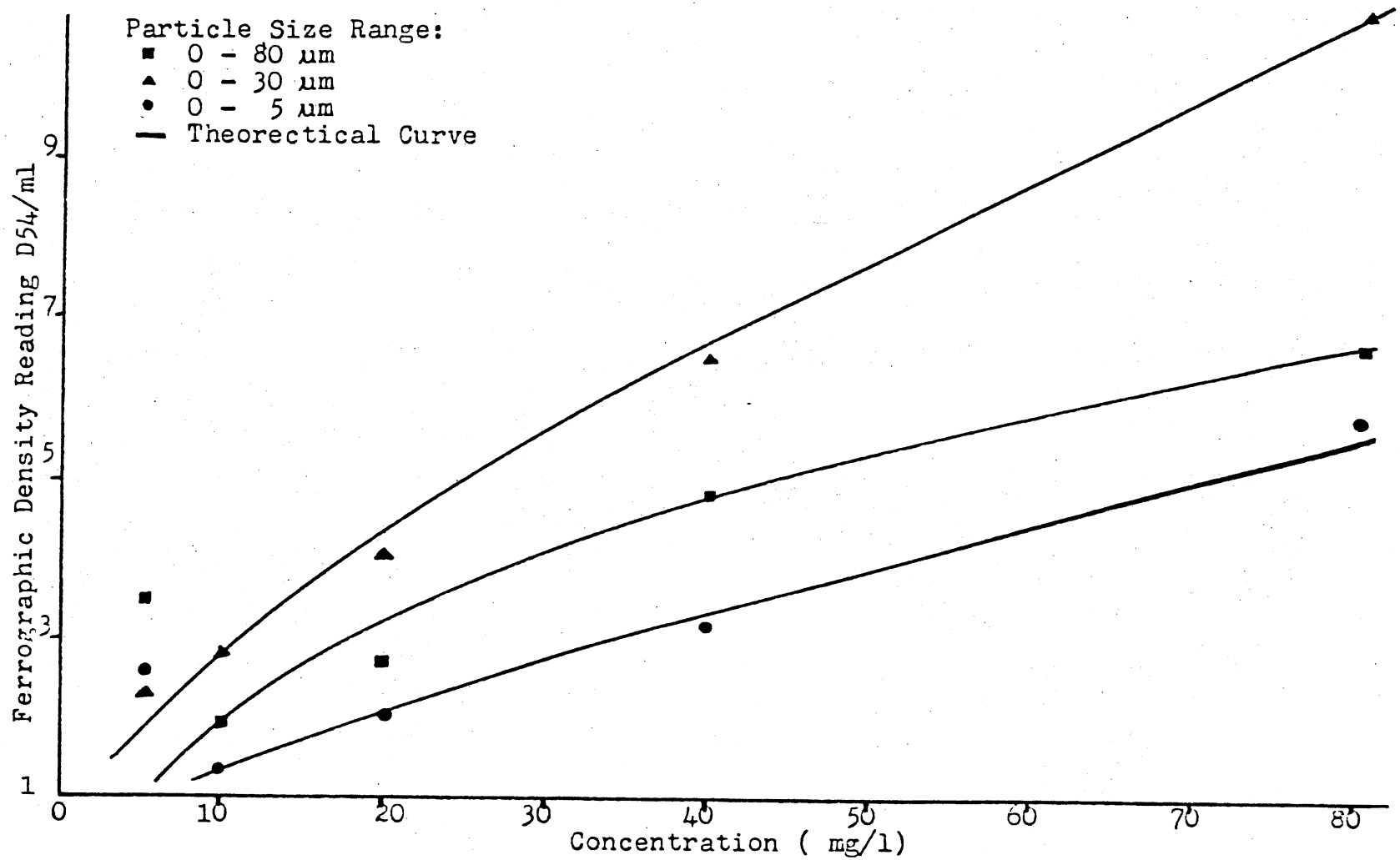

Figure 18. D54/ml vs Particle Concentration at Wedge Condition

TABLE III

PERFORMANCE EQUATION

Test Sequence	Fixed Parameter	Performance Equation	Coefficient of Deter
1 (1-1,2,3)	0- 5	$FD(54)=0.340C^{0.590}$	0.980
	0-30	$FD(54)=0.295C^{0.714}$	1.000
	0-80	$FD(54)=0.080C^{1.110}$	1.040
	20mg/l	$FD(54)=1.740D^{0.058}$	0.833
	40mg/l	$FD(54)=2.700D^{0.140}$	0.875
	80mg/l	$FD(54)=2.570D^{0.280}$	0.750
2 (2-1,2,3)	0- 5	$FD(54)=0.220C^{0.730}$	0.956
	0-30	$FD(54)=0.570C^{0.670}$	0.990
	0-80	$FD(54)=0.590C^{0.560}$	0.945

C: Contaminant concentration
D: Upper limit of particle cut size

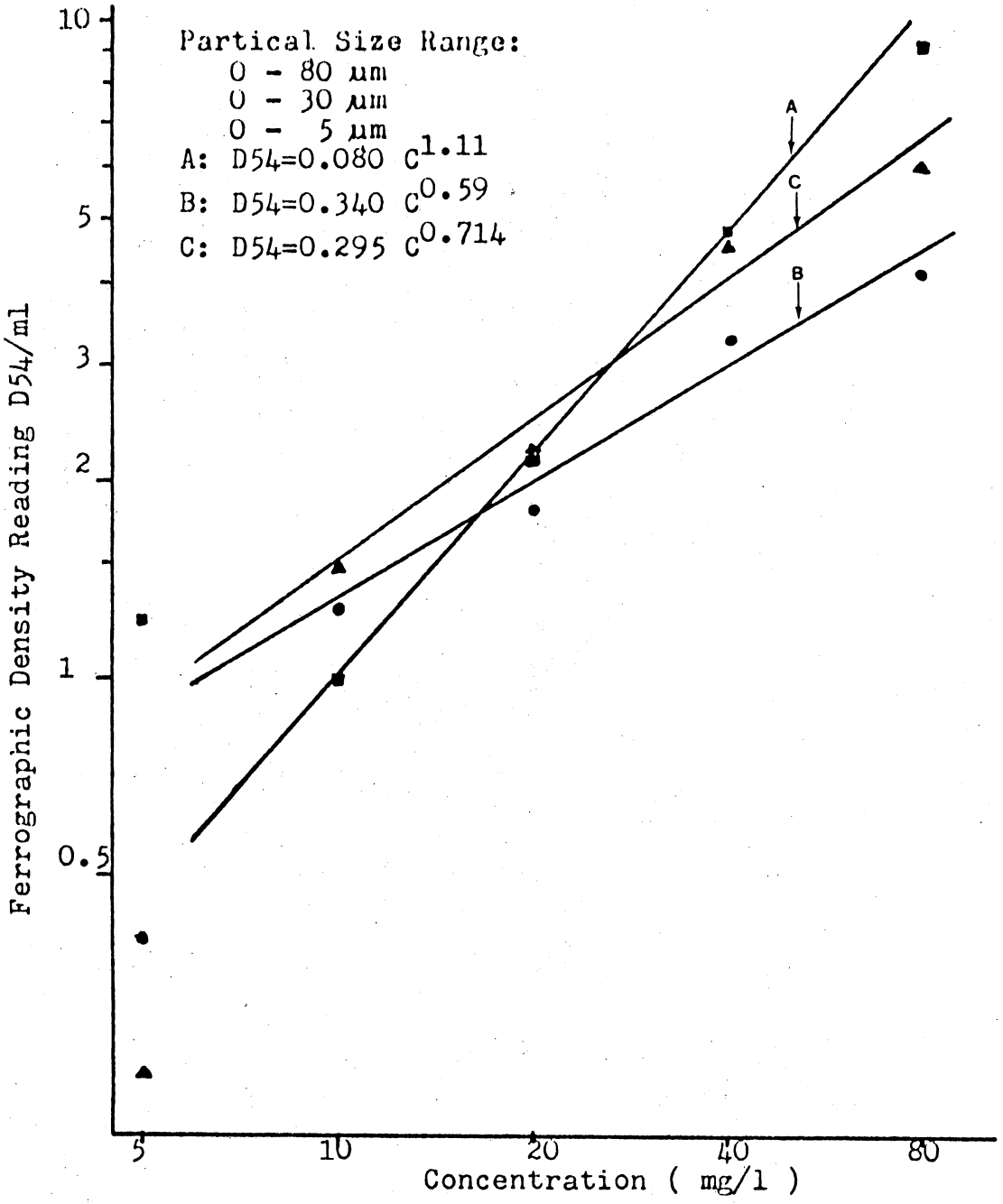

Figure 19. D54/ml vs Particle Concentration in Log-Log Scale at Normal Condition

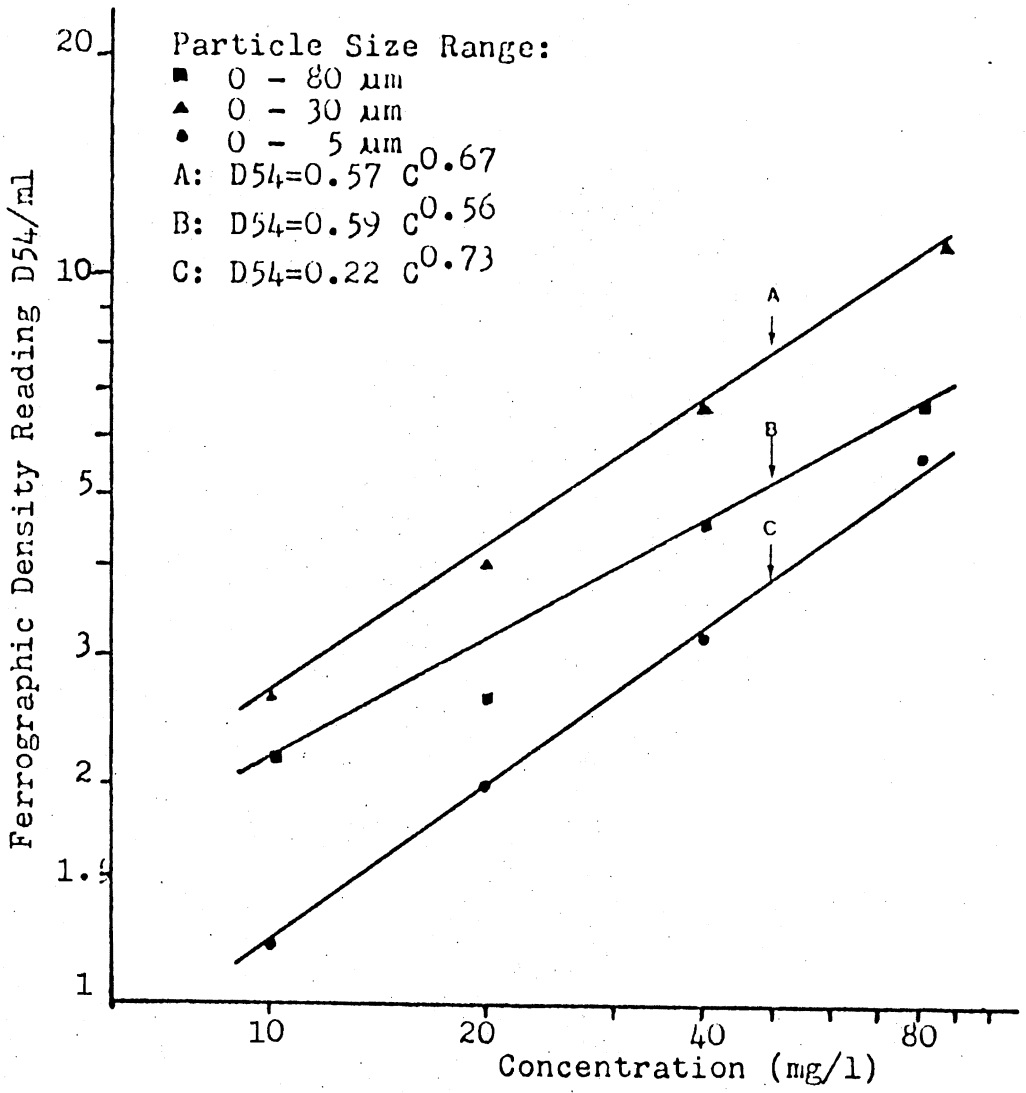

Figure 20. D54/ml vs Particle Concentration in Log-Log Scale at Wedge Condition

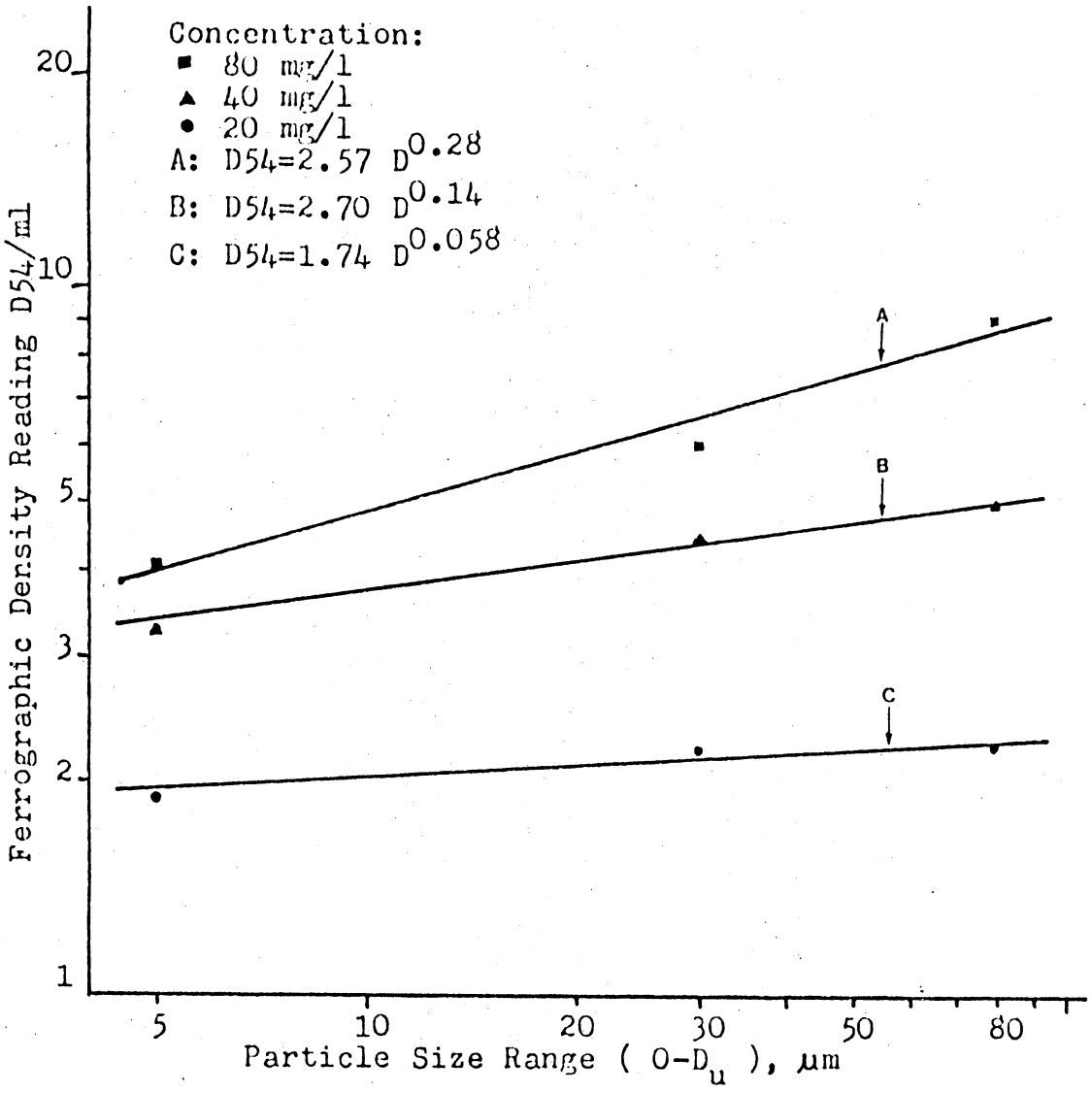

Figure 22. D54/ml vs Particle Size Range in Log-Log Scale at Normal Condition

Disscusion

As illustrated in Figure 17, wear debris density readings increase as abrasive particle size range increases at a fixed concentration level which is in agreement with the abrasive wear theories investigated in Chapter II. In Appendix C, in Figures 23-27 are presented a set of Ferrograms which show that density readings D54 on each 14 minutes sample. It should be noted that Ferrograms should not to be used to evaluate the wear rate except under similar test situations, such as the slide location and sample volumes.

A closer look of the debris in the high magnification microphotographs of Figures 28-32 reveals more detail. It was found that the least amount of debris was generated by the 0-5 micrometers cut dust, more by the 0-30 micrometers cut and the maximum by the 0-80 micrometers cut ACFTD. This fact suggests that the larger the abrasive particles in oil, the more the wear debris produced if the influence of various contamination levels were as expected -- the higher concentration the more the wear debris.

Furthermore, the characteristic curves converge rapidly in the low contaminate concentration. This implies that particle size distribution factor is insignificant at low contamination level.

The normalized density reading D54/ml obtained

from the Ferrogram of the sliding contact mechanism with the wedging effect, namely the size of the wearing surface clearance close to the particle upper size of ACFTD cut are shown in Figure 18, of particular interest here is the fact that a much higher amount of debris density was measured during the 0-30 micrometer exposure than either in the 0-5 on the 0-80 tests. This phenomenon agrees with the wedging action concept suggested in Chapter III.

Figure 22 depicts the results obtained by the particle counting technique. As can be seen from these figures, the trend of contaminant concentration build up during 0-5 and 0-80 tests are very similar, however, observations in the 0-30 tests have a significant difference. Furthermore, Figures 33-42 are Ferrograms of density readings obtained at the 54mm position. These magnified debris covered Ferrogram reveal that more wear debris were formed in the 0-30 test. This indicated that the wedging phenomena is indeed a property of sliding contact wear caused by abrasive particle in interfacing fluids.

Since the results obtained from the direct particle counting technique agree with the density measured through Ferrographic methods, it has been verified that Ferrography and Ferrographic-Wear models developed in this study are reliable.

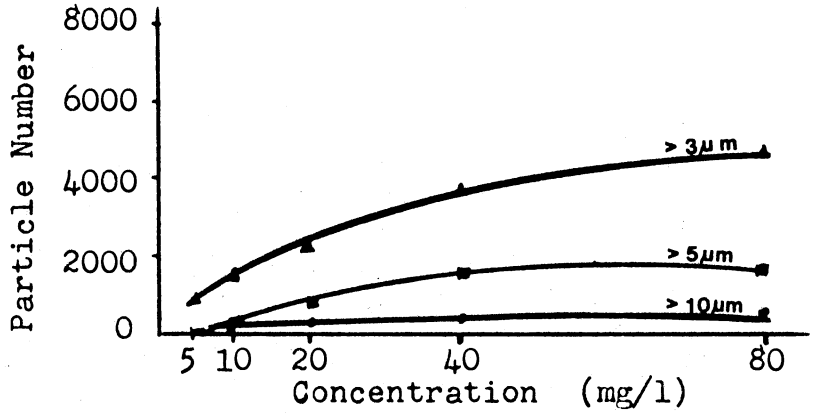

(a) 0-5 um exposed

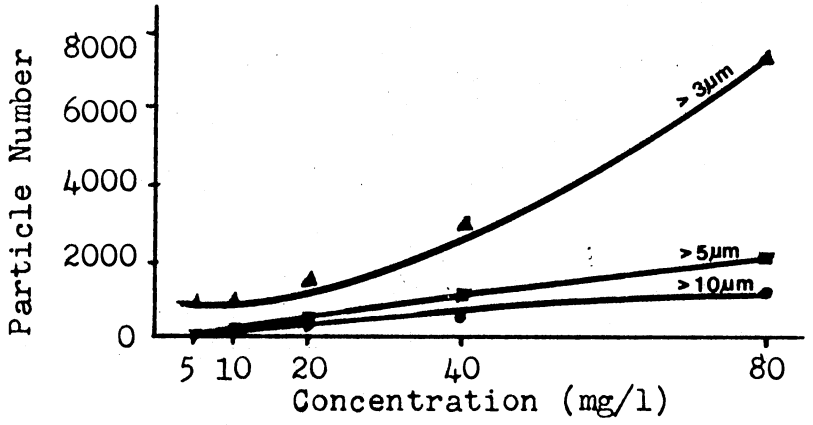

(b) 0-30 um exposed

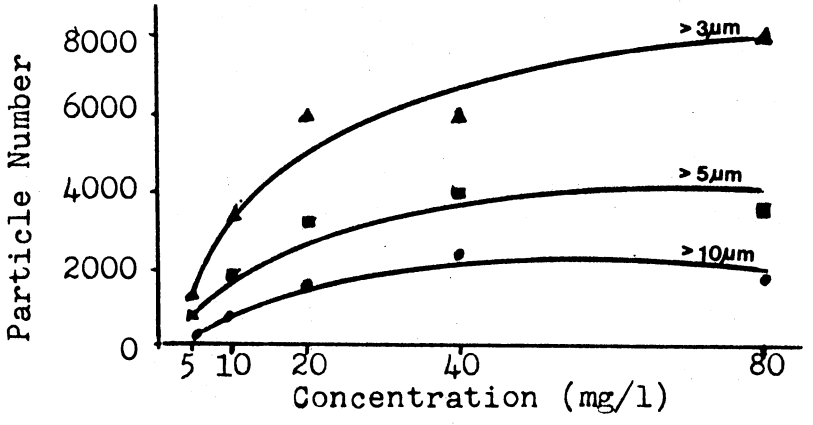

(c) 0-80 um exposed

Figure 22. Particle Count Analysis of Sliding Contact Wear Test

CHAPTER V

SUMMARY AND CONCLUSIONS

Summary

Usually, power is transferred between components through the frictional effect in mechanical systems. In order to reduce the damage caused by the wasteful but unavoidable frictional processes, lubricants are used to separate two wearing surfaces by a fluid film.

Users of machinery have realized the importance of lubrication in machine components. Unfortunately, most of them are not aware of the deterioration induced by the dirt particles in the lubricating oils. Moreover, due to the complexity of wear processes, the reported investigations are limited to qualitative description more than development of an analysis format for use either in the phenomena explainations or a form ready for use in realistic situations. This effect was based on the tribological wear theories and a non-intrusive analysis technique to further the knowledge of the sliding contact wear phenomenon caused by abrasive particle in interfacing fluids and develop Ferrographic-Wear models which can be used to solve the above mentioned problems.

Ferrography, used to assess the degree of contaminant induced wear in lubricated systems, was evaluated by correlating the D.R.. The correlation results showed that the Ferrography method accurately predicts the wear phenomena.

On the basis of electromagnetic principles and particle dynamic theories, a relation between the wear rate and the Ferrogram density reading was derived. This work was considered essential prior to the development of the Ferrographic-Wear models.

Particle size range and particle concentration in fluids are shown to be the critical parameters in this research.

The Ferrographic-Wear models showed that the Ferrogram debris density reading is a power function of the particle upper cut size and particle concentration respectively. The coefficients and exponents depend on the test conditions, but are constant in a fixed parameter situation. For example for a fixed particle size, the function governing the behaviour of the density reading and the contaminant concentration has a constant coefficient and exponent.

Wedging action should be considered as a property of sliding contact wear mechanism. It occurs when the clearance between two wearing surfaces have the same size as the upper cut size of contaminant particles. This

effect induces a significant increase in the amount of wear debris.

Tests were conducted to evaluate the Ferrographic-Wear models developed during this study. The test plan was formulated in such a manner that both the normal wear tests and the wedging wear tests could be performed. The extraneous abrasive particles used were those of ACFTD ranging from 0-5, 0-30, and 0-80 micrometer. This dust was entrained into the system according to a well-planed schedule.

Test results were obtained from the Ferrograms. Both numerical density readings, D54, and a magnified Ferrogram were obtained from the fluid samples. The numerical density readings, D54, were normalized for the same unit volume, normally using 1 milliliter and were analyzed statistically by means of the least squares curve fitting method to obtain the related performance equation sets.

Finally, the theoretical Ferrographic-Wear model was verified and was shown to have good agreement with the experimental data obtained from the different tests. This fact strongly demonstrated that the models developed in this study are adequate to predict the wear phenomena of abrasive particle induced by sliding contact mechanism wear.

Conclusion

From the research investigation described in the preceding chapters, several noteworthy conclusions can be listed as follows:

1. During the Ferrography evaluation study, it was noted that D54 is most responsive type of reading for sliding contact wear mechanism.
2. Based upon the electromagnetic principles and particle dynamic properties, the performance equation relating Ferrogram density reading FD(1) to wear rate (W) can be derived. It has the following form: $FD(1) = k_5 W$ where k_5 is a proportionality constant. This work can advance other Ferrographic-Wear studies.
3. Normalized density reading D54/ml is a power function in terms of the upper cut size of contaminant particles. This conclusion is applicable to all sliding contact wear mechanisms by setting other parameters constant, with the exception of those with wedging effects.
4. Normalized density reading D54/ml again is a power function in terms of particle concentration. This characteristic is applicable to all sliding contact wear mechanism by setting other parameters constant.
5. By means of the least square curve fitting method,

results obtained from the tests have been analyzed statistically in order to verify the Ferrographic-Wear models. The experimental results reveal good agreement to the theoretical Ferrographic-Wear models except in the low contamination concentration level. This is due to the fact that particle size distribution is not a significant factor in the low concentration range.

6. In this study, wedging phenomena is of particular interest. It not only provides an unusual increase in wear debris in the critical particle size range but also provides a good basis for the filter designers. This phenomenon implies that in dealing with the sliding contact mechanism, reducing the particle size range (at a give concentration) of the entrained contaminants may not decrease the component wear.
7. From this study, it is concluded that the wear mechanism can be analyzed by means of a non-intrusive oil analysis technique. Furthermore, the performance wear models developed through this technique have been verified adequately in predicting the wear phenomena in contaminant induced sliding wear mechanism. This indicated that this effort provides a feasible technique for use in wear phenomena analysis in realistic situations.

A SELECTED BIBLIOGRAPHY

1. Eyre, T.S. "Wear Characteristics of Metal." Tribology International, Vol. 9 (October, 1976), 203-212.

2. Lee, K.Z. "Tribology Engineering." Chinese Mechanical Engineer Handbook, II, Chapter 14 (1979), 1-2.

3. Winder, R.L. et al. "Valuable Results From Bearing Damage Analysis." Metal Progress, Vol. 112 (1977), 60-68.

4. Fitzsimmons, B., and H.D. Clevenger. The Effect of Contaminated Lubricants Upon Tapered Roller Bearing Wear. Paper No. P74-57, Eighth Annual Fluid Power Research Conference. Stillwater, Oklahoma: Oklahoma State University, 1974.

5. Fitzsimmons, B., and B.J. Cave. Lubricant Contaminant and Their Effects on Bearing Performance. Paper 750583. New York, N. Y.: Society of Automotive Engineers, 1975.

6. Becstrom, J.A. "A Ferrographic Wear Study - The Effect of Particulate Contaminated Lubricant on Wear Rates of Ball Bearings." The BFPR Journal, Vol. 13 (1980), 371-376.

7. Ku, P.M. "Gear Failure Modes - Importance of Lubrication and Mechanics." ASLE TRAN., Vol. 19 (1976), 239-249.

8. Seifert, W.W. and V.C. Westcott. "A Method for the Study of Wear Particles in Lubricating Oil." Wear, Vol. 21 (1972), 27-43.

9. Jones, W.R. et al. "Ferrographic Analysis of Wear Debris Generated in Sliding Elastrohydrodynamic Contact." ASLE TRAN., Vol. 21 (1977), 181-190.

10. Tessman, R.K. "Non-Intrusive Analysis of Contaminant Wear in Gear Pump Through Ferrography." (Unpublished Doctoral Dissertation, Oklahoma State University, 1977.)

11. Scott, D. et al. "Ferrography - An Advanced Design Aid for the 80's." Wear, Vol. 34 (1975), 251-260.

12. Czichos, H. Tribology - A System Approaches to the Science and Technology of Friction, Lubrication and Wear. New York, N. Y.: Elsevier Scientific Publishing Company, 1978.

13. Peterson, M.B. "Wear Testing Objectives and Approaches." Source Book on Wear Control Technology. Metal Parks, Ohio: American Society for Metals, 1978, 40-48.

14. Halling, J. Principles of Tribology. New York, N. Y. : The Maemillan Press Ltd., 1975.

15. Rabinowicz, E. Friction and Wear of Materials. New York, N. Y.: John Weley and Sons, 1965.

16. Krushchov, K.K., and M.A. Babichev. "Investigation of the Resistance of Metals to Abrasion as Influence by the Hardness of the Abrasive." Friction and Wear in Machinery, Vol. 11 (1956), 19-26.

17. Nathan, G.K., and W.J.D. Jones. "Influence of the Hardness of the Abrasive on the Abrasive Wear of Metals." Process Institute of Mechanical Engineers, Vol. 181 (1966), 215-221.

18. Richardson, R.C.D. "The Wear of Metals by Relatively Soft Abrasives." Wear, Vol. 11 (1968), 245-275.

19. Truscott, G.F. "A Literature Survey on Abrasive Wear in Hydraulic Machinery." Wear, Vol 20 (1972), 29-51.

20. Rabinowicz, E. et al. "A Study of Abrasive Wear Under Three-Body Conditions." Wear, Vol. 4 (1961), 345-355.

21. Sin, H. et al. "Abrasive Wear Mechanism and the Grit Size Effect." Wear, Vol. 55 (1979), 163-190.

22. Babichev, M.A. "Investigation of the Abrasive Wear of Metals by the Brinell Method." Friction and Wear in Machinery, Vol. 12 (1956), 1-29.

23. Larsen-Badse, J. "Influence of Grit Diameter and Specimen Size on Wear During Sliding Abrasion." Wear, Vol. 12 (1968), 35-53.

24. Rabinowicz, E., and A. Mutis. "Effect of Abrasive Particle Size on Wear." Wear, Vol. 8 (1965), 381-390.

25. Wear in Fluid Power Systems. Final Report, Contract No. N00010-75-C-1157, Arlington, V. A.: Office of Naval Research, 1979.

26. Tao, F.F. et al. "An Experimental Study of the Wear Caused by Loose Abrasive Particles in Oils." ASLE TRAN., Vol. 13 (1969), 169-178.

27. Lomakin, V.S. "Investigation of Wear of Sleeves and Piston Rings of Mud Pumps." Friction and Wear in Machinery, Vol. 12 (1956), 39-69.

28. Moore, M.A. "Areview of Two-Body Abrasive Wear." Wear, Vol. 27 (1974), 1-17.

29. Khruschov, M.M. "Principles of Abrasive Wear." Wear, Vol. 28 (1974), 69-88.

30. Finnie, I. "Erosion of Surfaces by Solid Particles." Wear, Vol. 3 (1960), 71-83.

31. Tilly, G.P. "A Two Stage Mechanism of Ductile Erosion." Wear, Vol. 23 (1973), 87-96.

32. Friction and Wear Devices. Park Ridge, Illinois: American Society of Lubrication Engineers, 1976.

33. Chu, J. "Development of A Bench Type Contaminant Wear Test." The FRH Journal, Vol. 2 (1980), 121-127.

34. Bensch, L.E. "An Investigation of the Variance of AC Test Dust." The BFPR Journal, Vol. 21 (1976), 1-5.

35. Ruff, A.W. "Characterization of Debris Particles Recovered From Wearing Systems." Wear, Vol. 42 (1977), 49-62.

36. The Survivability Characteristics of Fluid Power Components in Contaminated Environment. Annual Report, Contract No. N00014-75-C-1157, Arlington, V. A.: Office of Naval Research, 1976.

37. Senholzi, P.B., and C.R. Bowen. "Oil Analysis Research." Proceedings of the National Conference on Fluid Power., Vol. XXX (1976), 355-365.

38. Effect of Lubricant Contaminants on Wear Rates of Lubricated Components. Final Report, Contract No. NAVY N68335-76-C-2780, Washington, D. C.: Naval Air Engineering Center, 1978.

39. Nair, K.S. "The Physics of Analytic Ferrography." (Unpublished M.S. Thesis, Oklahoma State University, 1980.)

40. Fitch, E.C. An Encyclopedia of Fluid Contamination Control. Washington, D. C.: Hemisphere Publishing Corporation, 1980.

41. The Survivability Characteristics of Fluid Power Components in Contaminated Environments. Final Report, Contract No. N00014-75-C-1157, Arlington, V. A.: Office of Naval Research, 1979.

APPENDIX A

BREAK-IN PROCEDURE

The suggested Break-In procedure in the sliding wear tests are as follos:

1. Install oil-wetted specimen set (spool and bores) in mechanism.
2. Connect drive mechanism and check for proper alignment.
3. Operate stand until proper oil temperature is achieved, set proper flow through mechanism, and set pressure to 25% of test pressure.
4. Activate mechanism and operate for 15 minutes.
5. Increase pressure by 25% of test pressure and operate for 15 minutes.
6. Repeat 5 until test pressure is achieved.
7. Operate at full test pressure for one hour.

APPENDIX B

THE LEAST SQUARE CURVE FITTING METHOD APPLIED IN A LOG-LOG FUNCTION

Concerning a log-log function, it can be expressed as:

$$\log W = \log a + b \log D \tag{B-1}$$

or $$W = a\, D^{b} \tag{B-2}$$

The first step to apply the least square curve fitting technique to this non-linear function is to convert suitable variables to reduce the primary function to a "linear relationship", and then follow the steps used to handle the conventional linear system problems. Details shown as follows:

$$\log W = \log a + b \log D \tag{B-3}$$

Let $\log W = Y$, $\log a = a_o$, $b = a_1$, $\log D = X$
then Equation (B-3) reduces to

$$Y = a_o + a_1 X \tag{B-4}$$

Now the performance equations for linear system can be employed to solve Equation (B-4). That is

$$\Sigma Y = a_o N + a_1 \Sigma X \tag{B-5}$$

$$\Sigma XY = a_o \Sigma X + a_1 \Sigma X^2 \tag{B-6}$$

or $$a_o = \frac{(\Sigma Y)(\Sigma X^2)-(\Sigma X)(\Sigma XY)}{N\Sigma X^2 - (\Sigma X)^2} \tag{B-7}$$

$$a_1 = \frac{N\Sigma XY - (\Sigma X)(\Sigma XY)}{N\Sigma X^2 - (\Sigma X)^2} \qquad \text{(B-8)}$$

where: N is the sampling number.

By Equation (B-7), (B-8), and (B-3), then the desired curve appears.

Also, the coefficient of determination r^2 is defined as

$$r^2 = \Sigma\,(Y_{est.} - \bar{Y})^2 / \Sigma (Y - \bar{Y})^2 \qquad \text{(B-9)}$$

where: $Y_{est.}$ = estimated value

$\bar{Y}$ = mean value

Y = observed value

APPENDIX C

FERROGRAMS

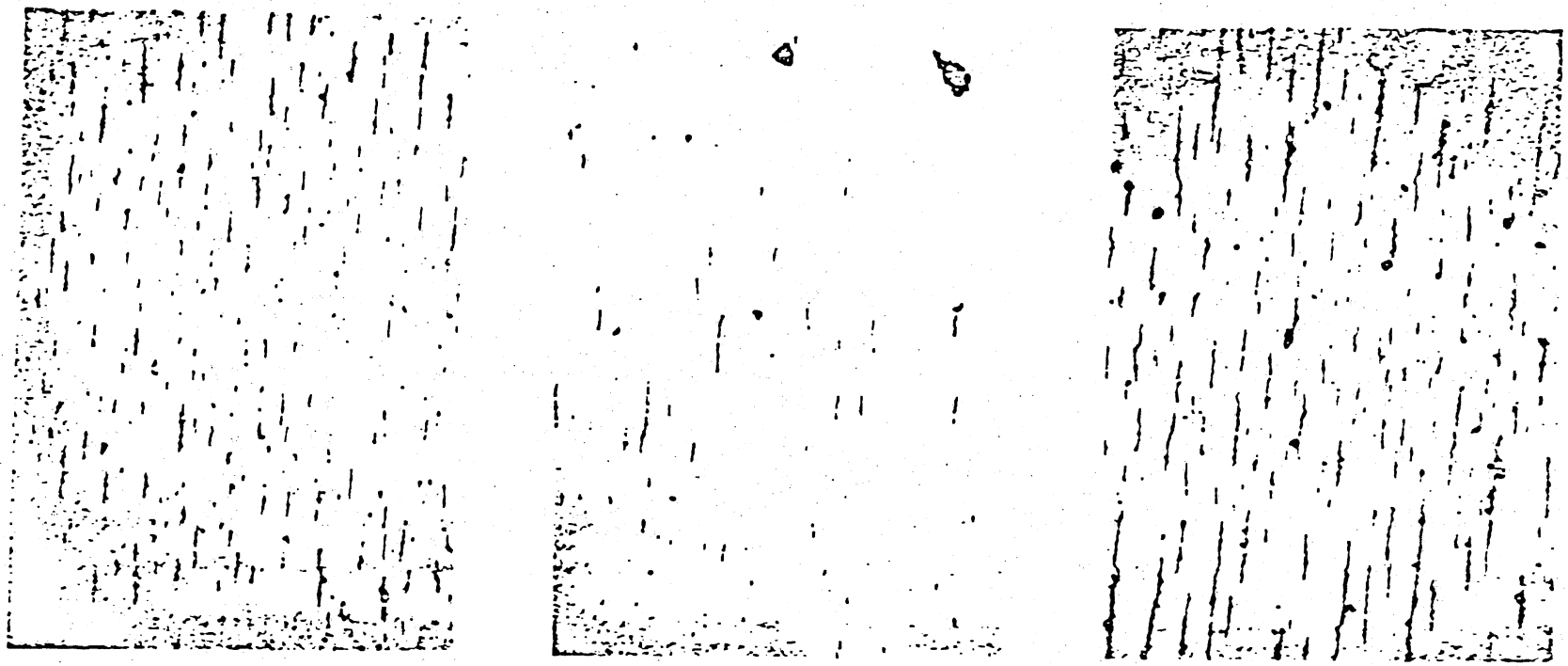

(a) 0-5 μm, V = 12 ml (b) 0-30 μm, V = 12 ml (c) 0-80 μm, V= 6 ml

Figure 23. Ferrograms of Wear Debris (54mm) From Sliding Mechanism After Exposure to 5 mg/l of Contaminant (magnification = 100X), Normal Condition.

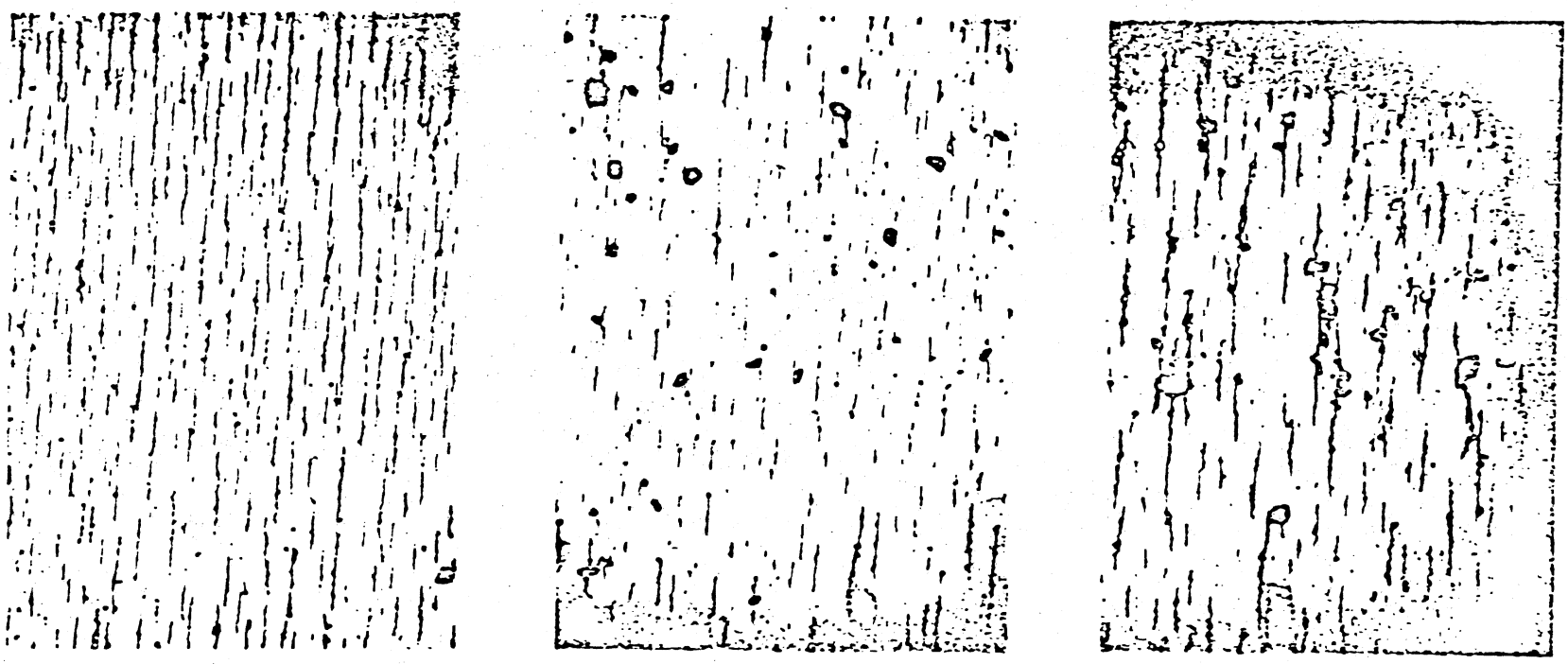

(a) 0-5 µm, V = 12ml (b) 0-30 µm, V = 12ml (c) 0-80 µm, V = 12ml

Figure 24. Ferrograms of Wear Debris (54mm) From Sliding Mechanism After Exposure to 10 mg/l of Contaminant (magnification = 100X). Normal Condition.

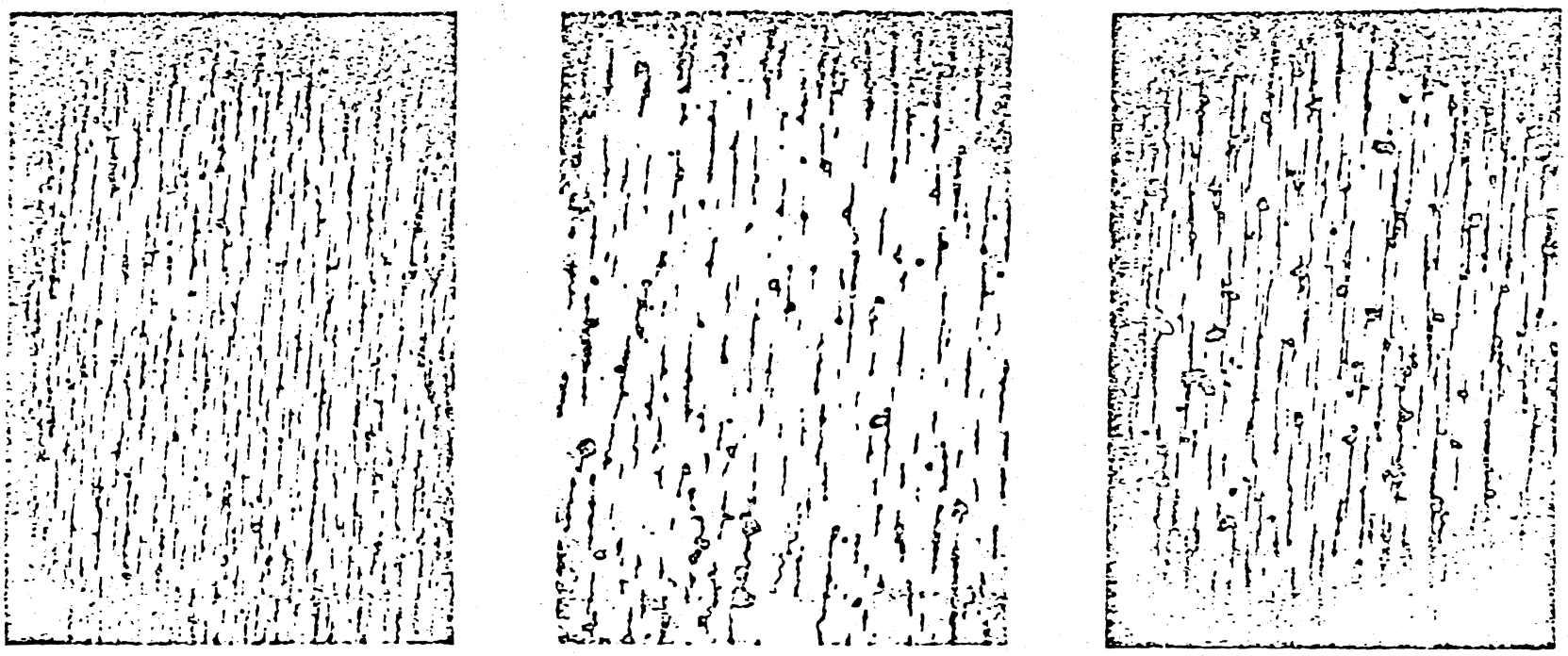

(a) 0-5 µm, V = 12 ml (b) 0-30 µm, V = 6 ml (c) 0-80 µm, V = 12 ml

Figure 25. Ferrograms of Wear Debris (54mm) From Sliding Mechanism After Exposure to 50 mg/l of Contaminant (magnification = 100X), Normal Condition.

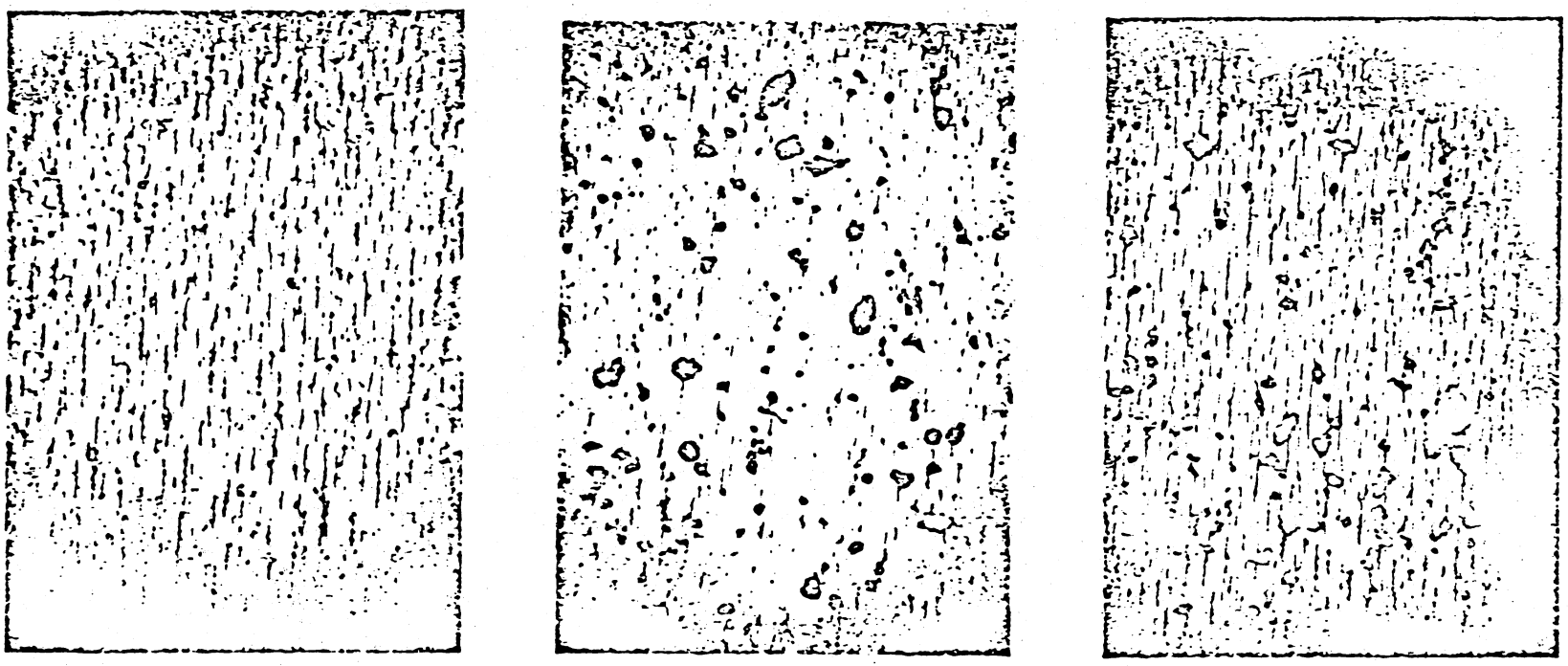

(a) 0-5 µm, V = 6 ml (b) 0-30 µm, V = 6 ml (c) 0-80 µm, V = 6 ml

Figure 26. Ferrograms of Wear Debris (54mm) From Sliding Mechanism After Exposure to 40 mg/l of Contaminant (magnification = 100X), Normal Condition.

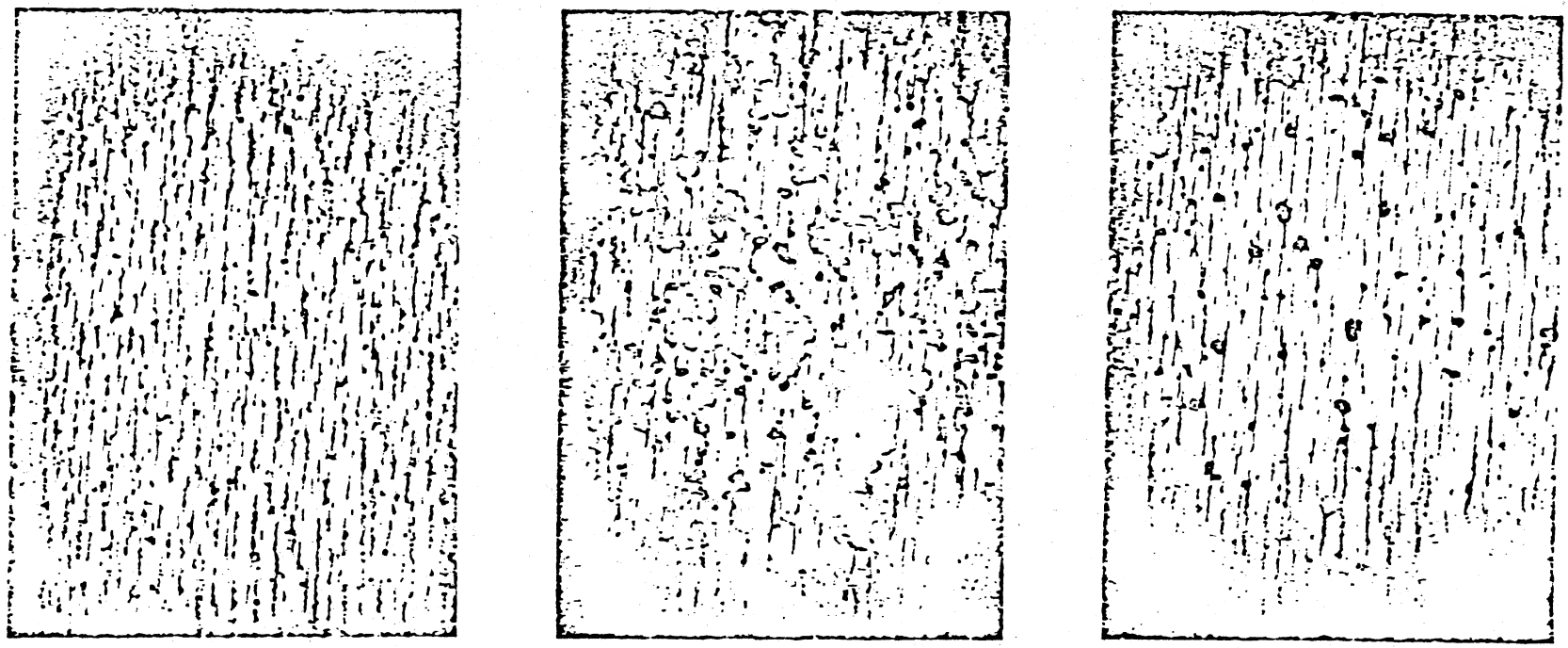

(a) 0-5 μm, V = 6 ml (b) 0-30 μm, V = 6 ml (c) 0-80 μm, V = 3 ml

Figure 27. Ferrograms of Wear Debris (54mm) From Sliding Mechanism After Exposure to 80 mg/l of Contaminant (magnification = 100X), Normal Condition.

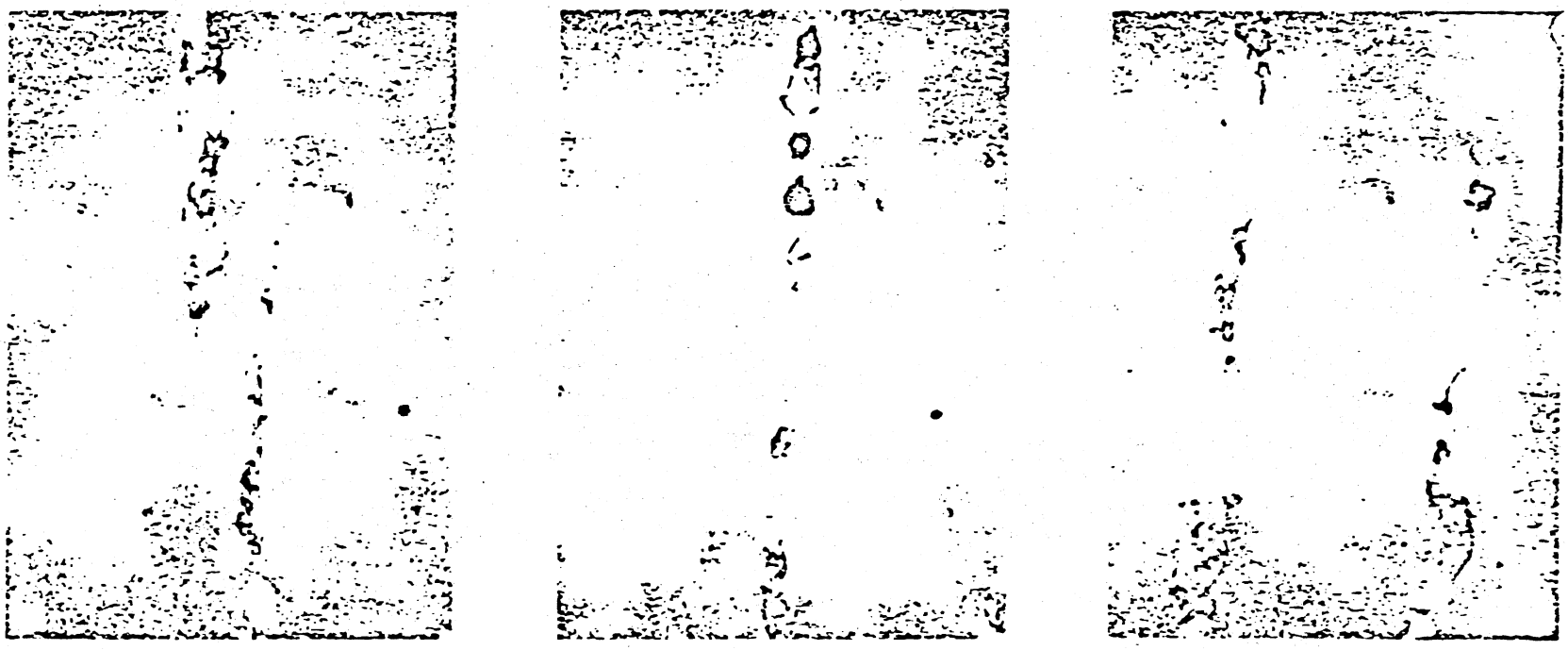

(a) 0-5 µm, V = 12 ml (b) 0-30 µm, V = 12 ml (c) 0-80 µm, V = 6 ml

Figure 28. Ferrograms of Wear Debris (54mm) From Sliding Mechanism After Exposure to 5 mg/l of Contaminant (magnification = 1000X), Normal Condition.

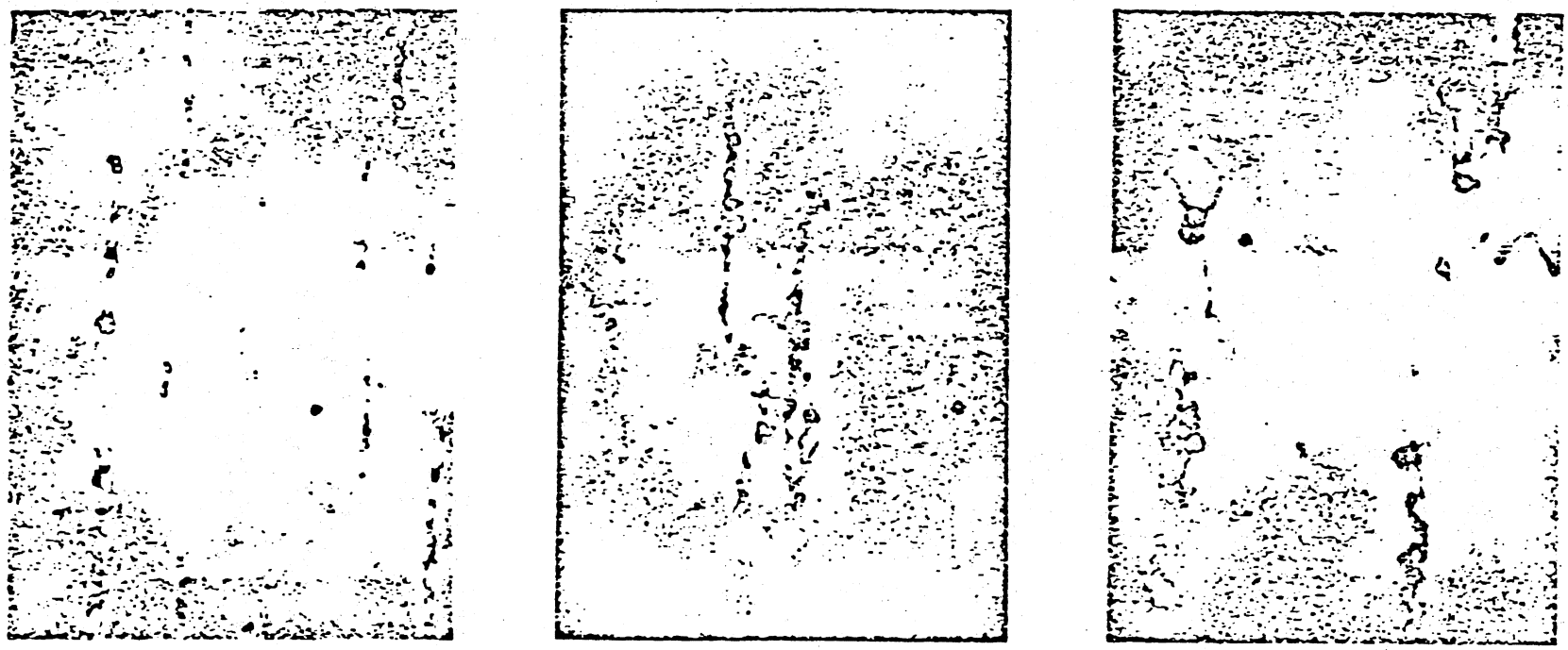

(a) 0-5 μm, V = 12 ml (b) 0-30 μm, V = 12 ml (c) 0-80 μm, V = 12 ml

Figure 29. Ferrograms of Wear Debris (54mm) From Sliding Mechanism After Exposure to 10 mg/l of Contaminant (magnification = 1000X), Normal Condition.

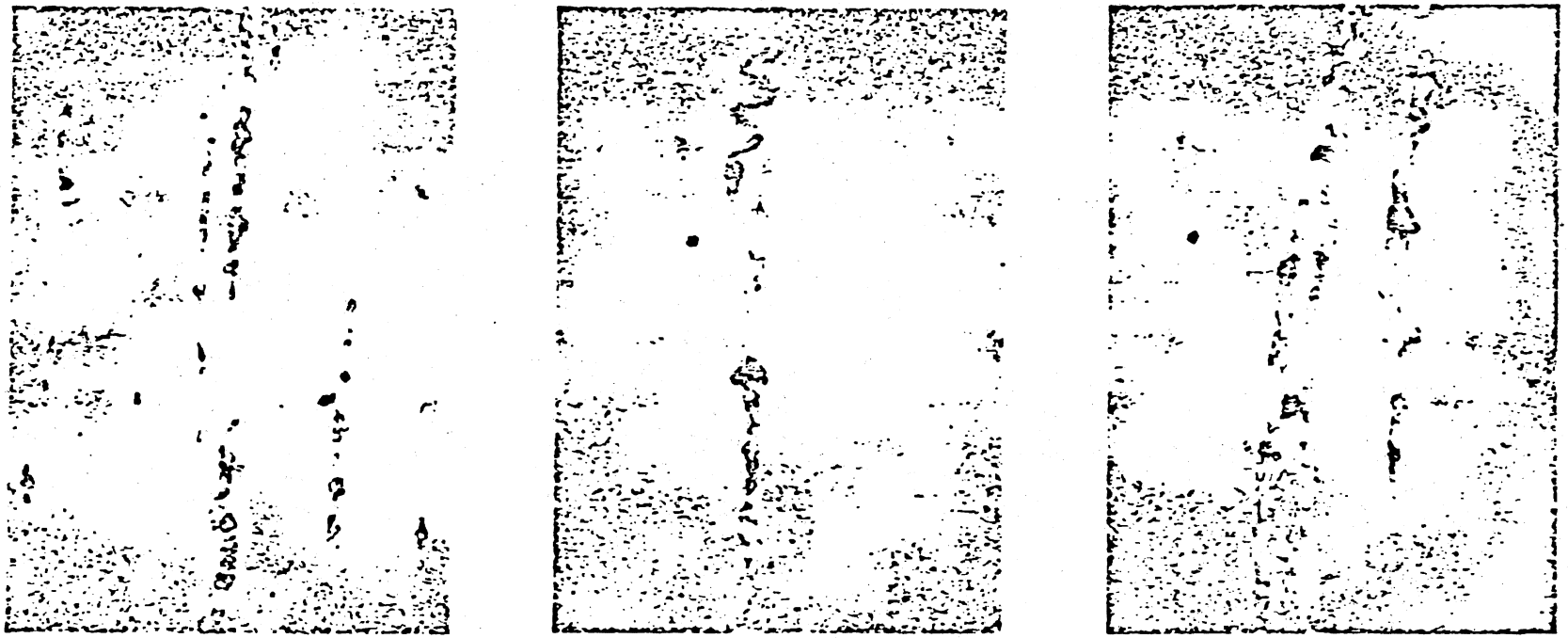

(a) 0-5 µm, V = 12 ml (b) 0-30 µm, V = 6 ml (c) 0-80 µm, V = 12 ml

Figure 30. Ferrograms of Wear Debris (54mm) From Sliding Mechanism After Exposure to 20 mg/l of Contaminant (magnification = 1000X), Normal Condition.

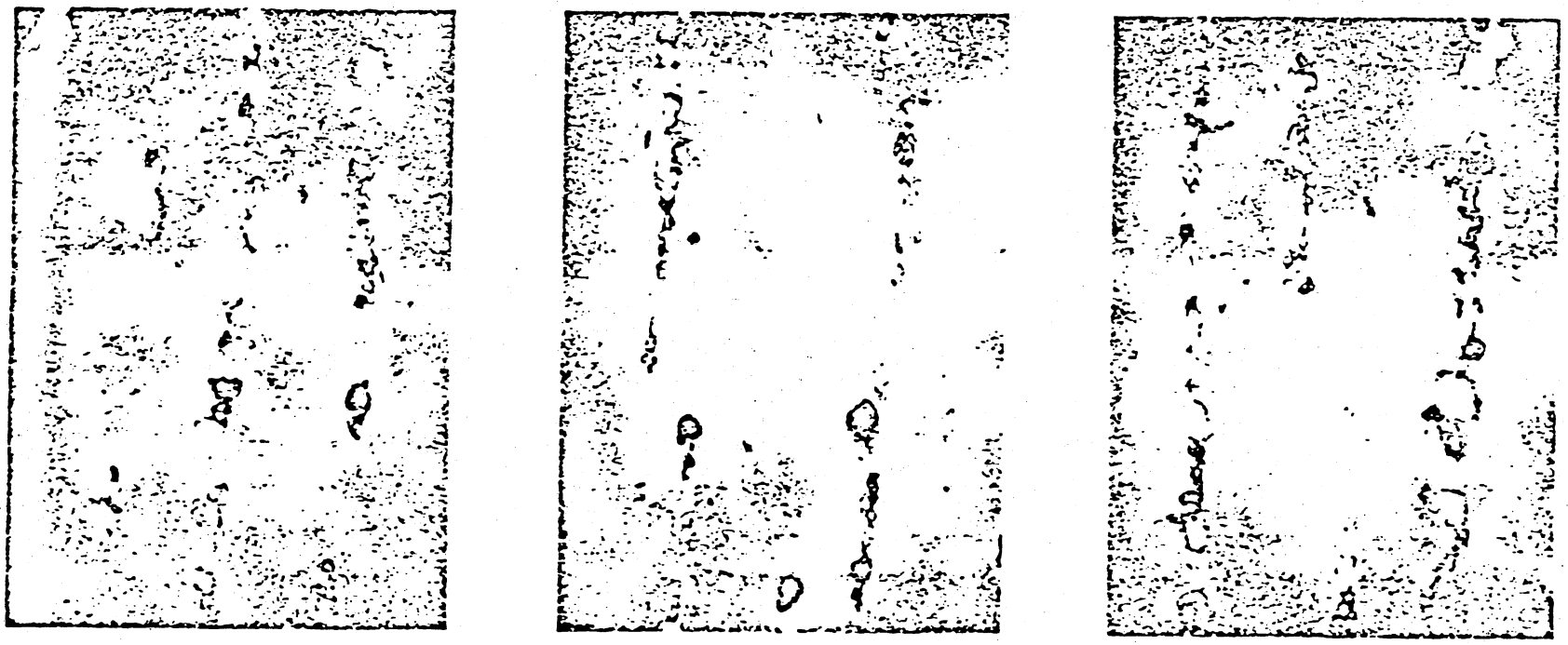

(a) 0-5 µm, V = 6 ml (b) 0-30 µm, V = 6 ml (c) 0-80 µm, V = 6ml

Figure 31. Ferrograms of Wear Debris (54mm) From Sliding Mechanism After Exposure to 40 mg/l of Contaminant (magnification = 1000X), Normal Condition.

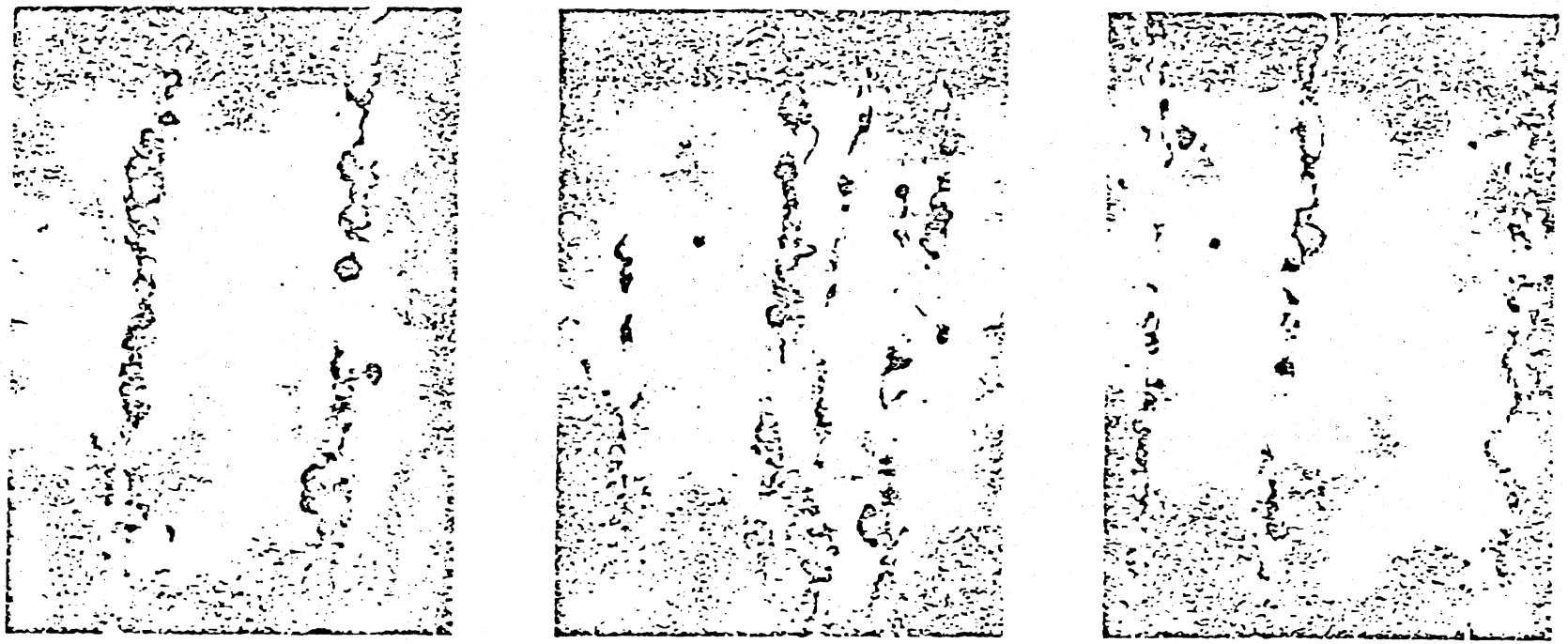

(a) 0-5 µm, V = 6 ml (b) 0-30 µm, V = 6 ml (c) 0-80 µm, V = 3 ml

Figure 32. Ferrograms of Wear Debris (54mm) From Sliding Mechanism After Exposure to 80 mg/l of Contaminant (magnification = 1000X), Normal Condition.

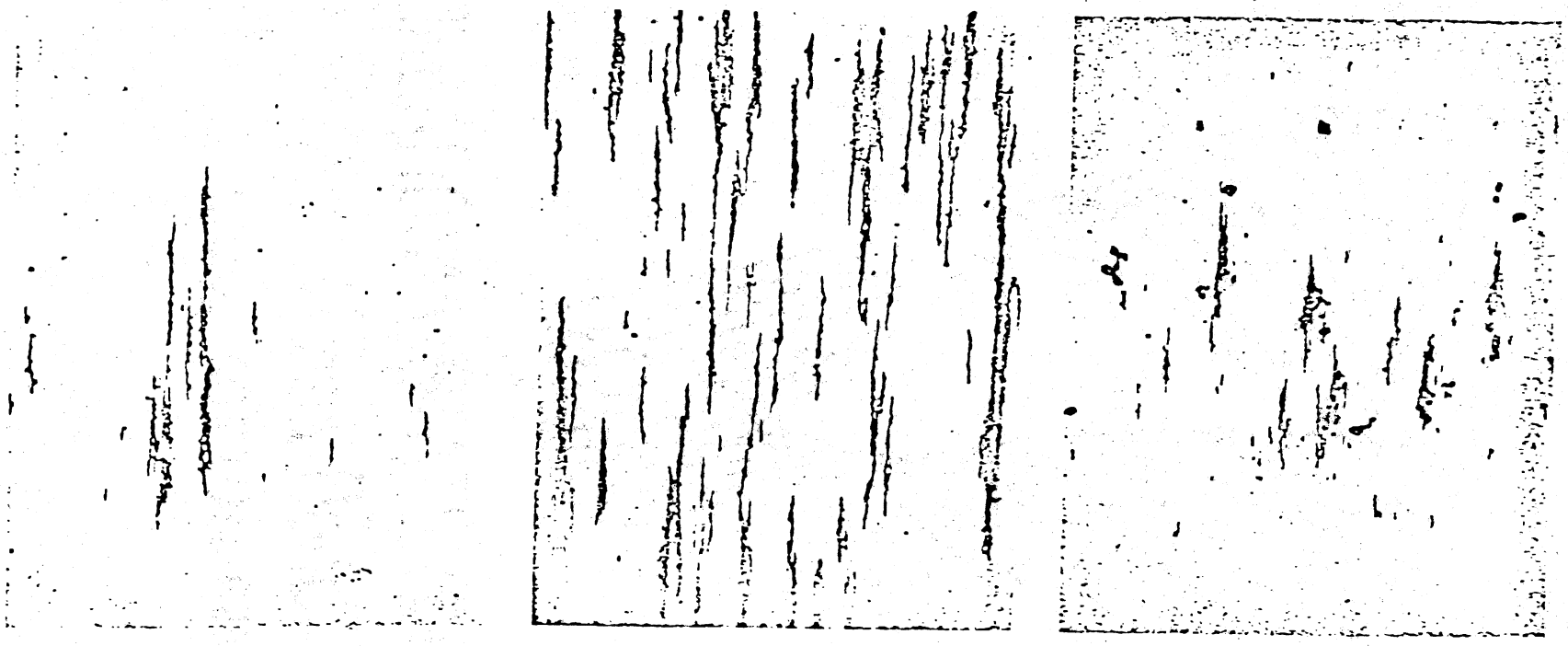

(a) 0-5 µm (b) 0-30 µm (c) 0-80 µm

Figure 33. Ferrograms of Wear Debris (54mm) From Sliding Mechanism After Exposure to 5 mg/l of Contaminant (magnification = 100X), Wedge Condition.

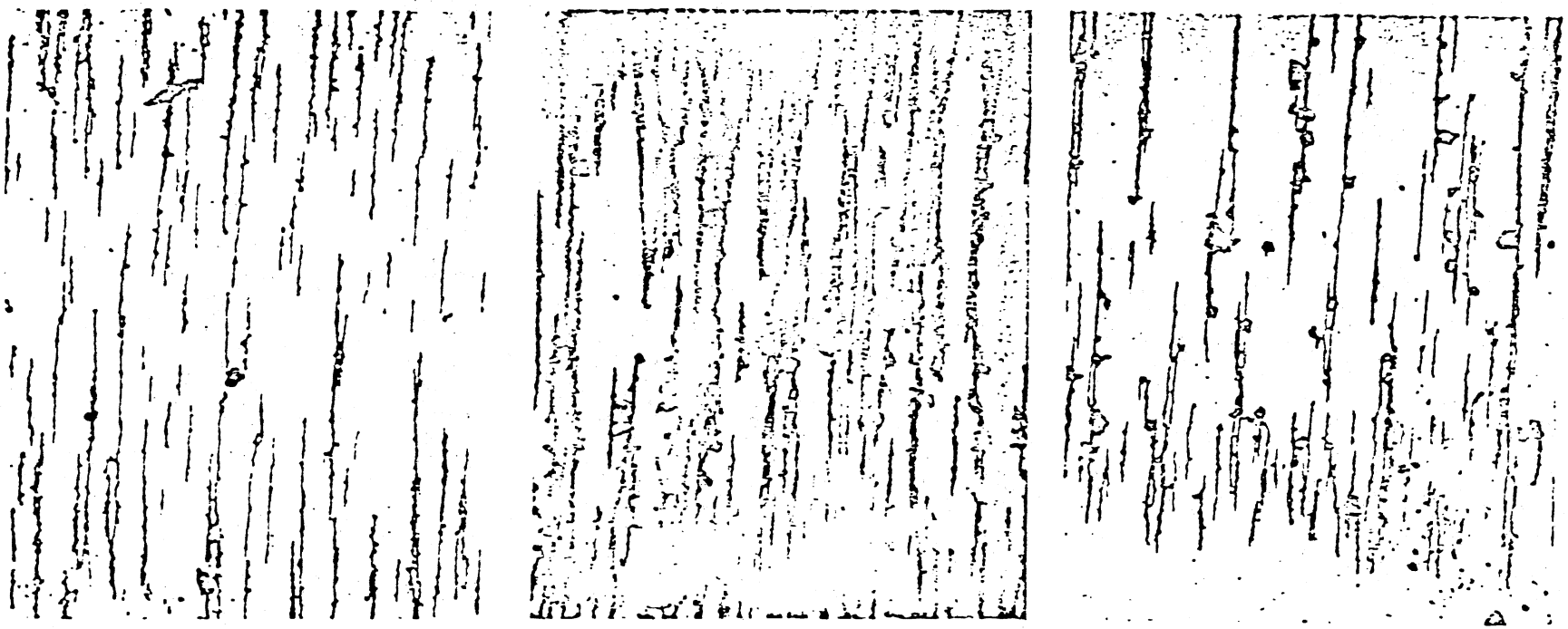

(a) 0-5 µm (b) 0-30 µm (c) 0-80 µm

Figure 34. Ferrograms of Wear Debris (54mm) From Sliding Mechanism After Exposure to 10 mg/l of Contaminant (magnification = 100X), Wedge Condition.

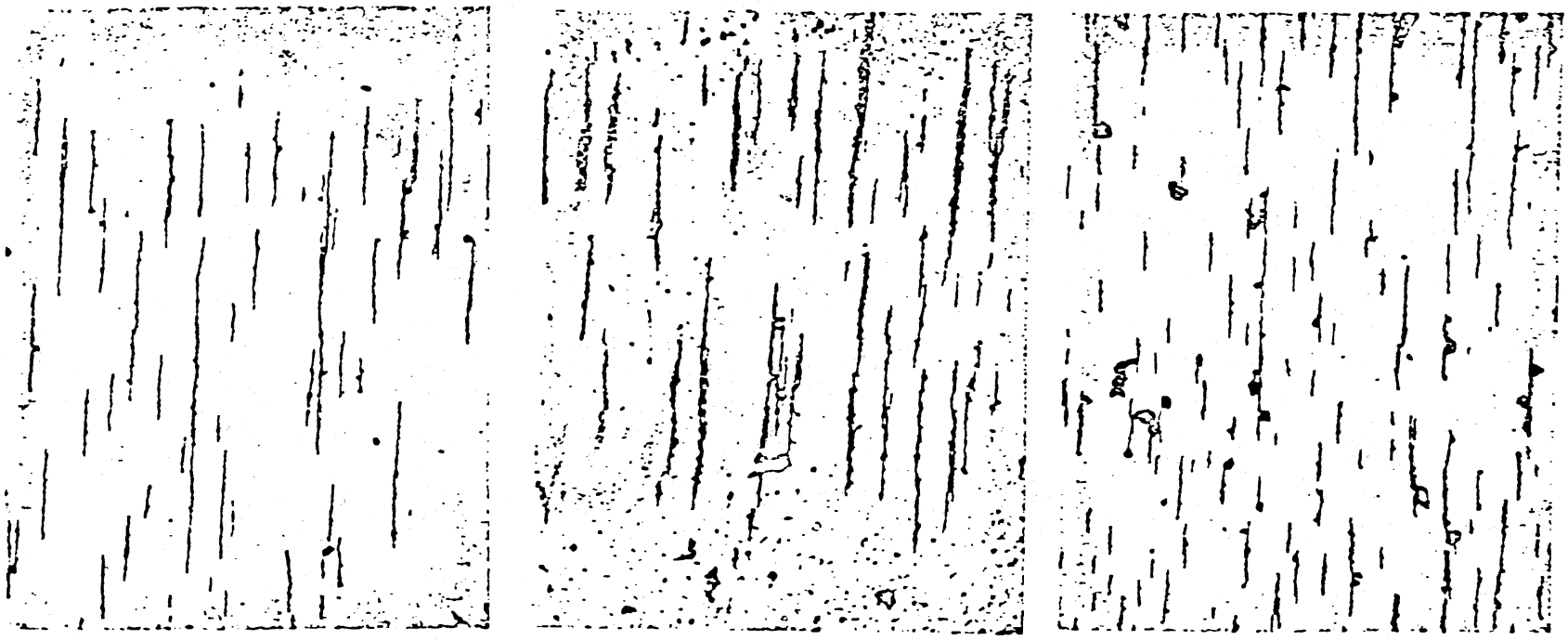

(a) 0-5 µm (b) 0-30 µm (c) 0-80 µm

Figure 35. Ferrograms of Wear Debris (54mm) From Sliding Mechanism After Exposure to 20 mg/l of Contaminant (magnification = 100X), Wedge Condition.

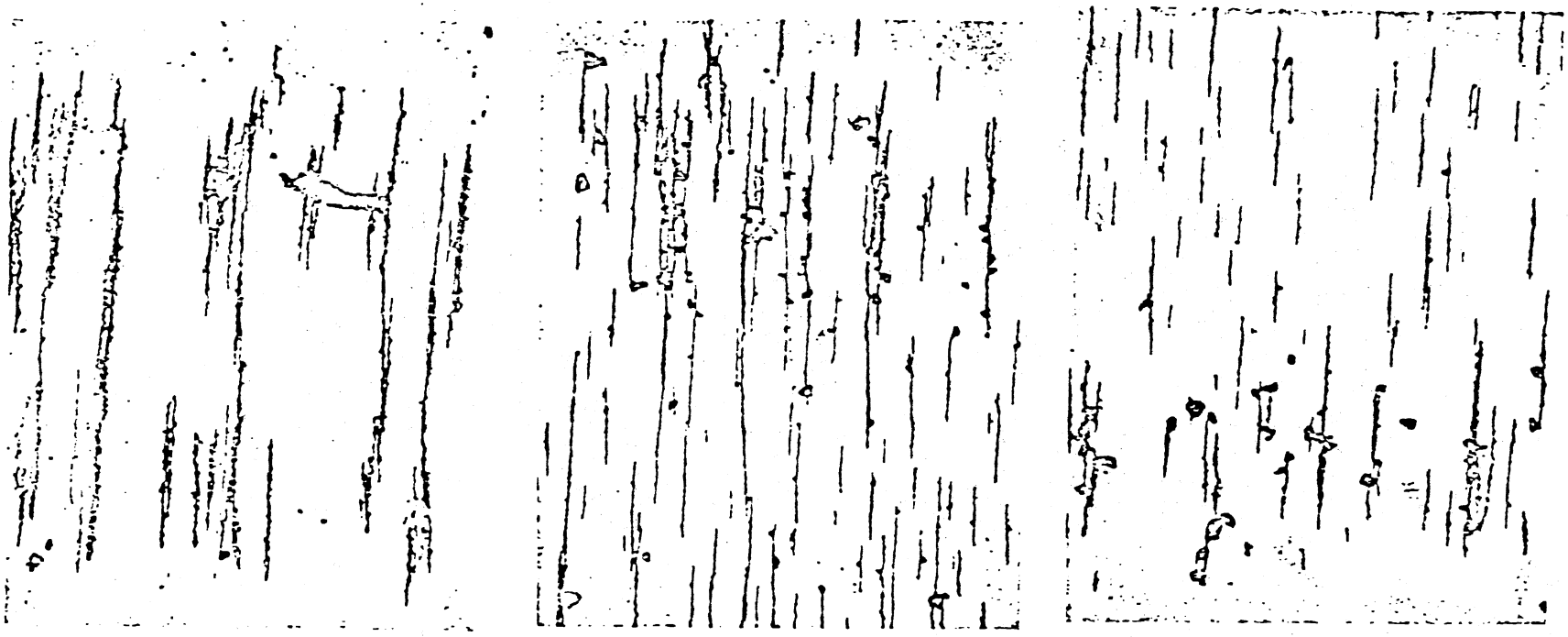

(a) 0-5 μm (b) 0-30 μm (c) 0-80 μm

Figure 36. Ferrograms of Wear Debris (54mm) From Sliding Mechanism After Exposure to 40 mg/l of Contaminant (magnification = 100X), Wedge Condition.

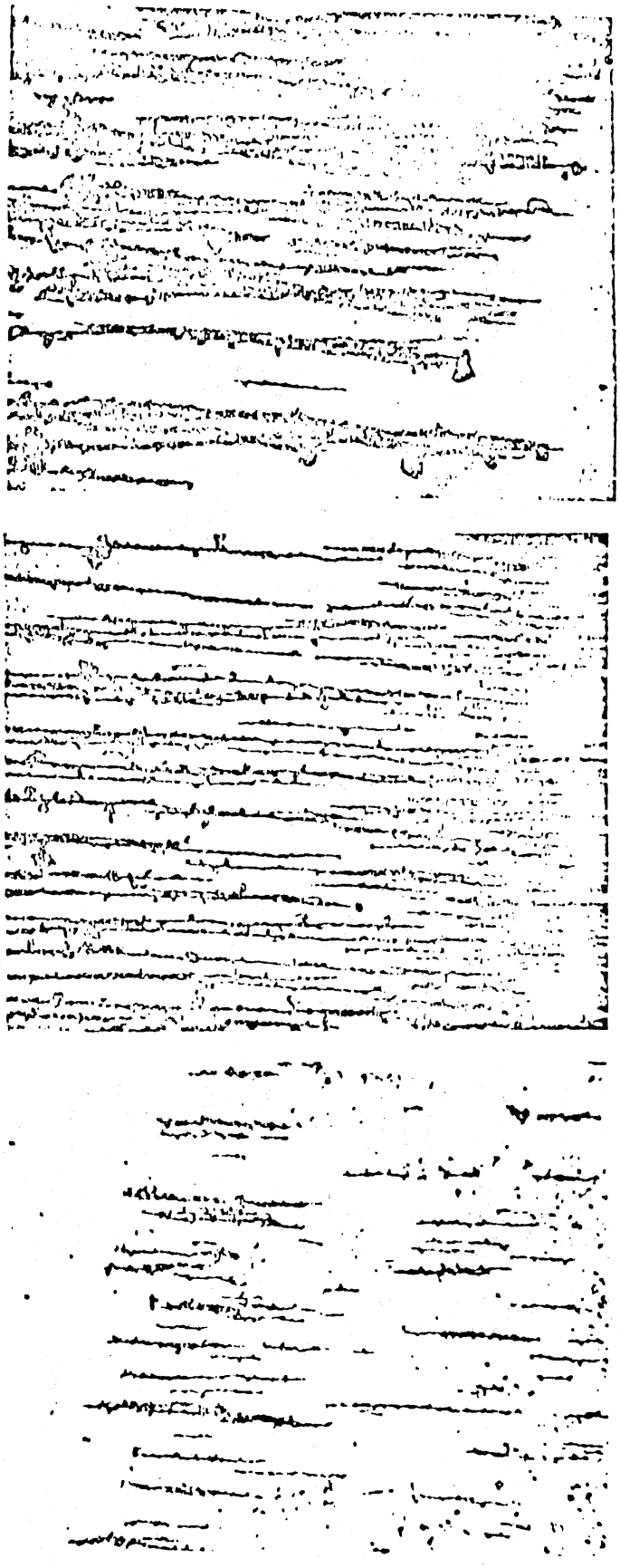

(a) 0-5 μm (b) 0-30 μm (c) 0-80 μm

Figure 37. Ferrograms of Wear Debris (54mm) From Sliding Mechanism After Exposure to 80 mg/l of Contaminant (magnification = 100X), Wedge Condition.

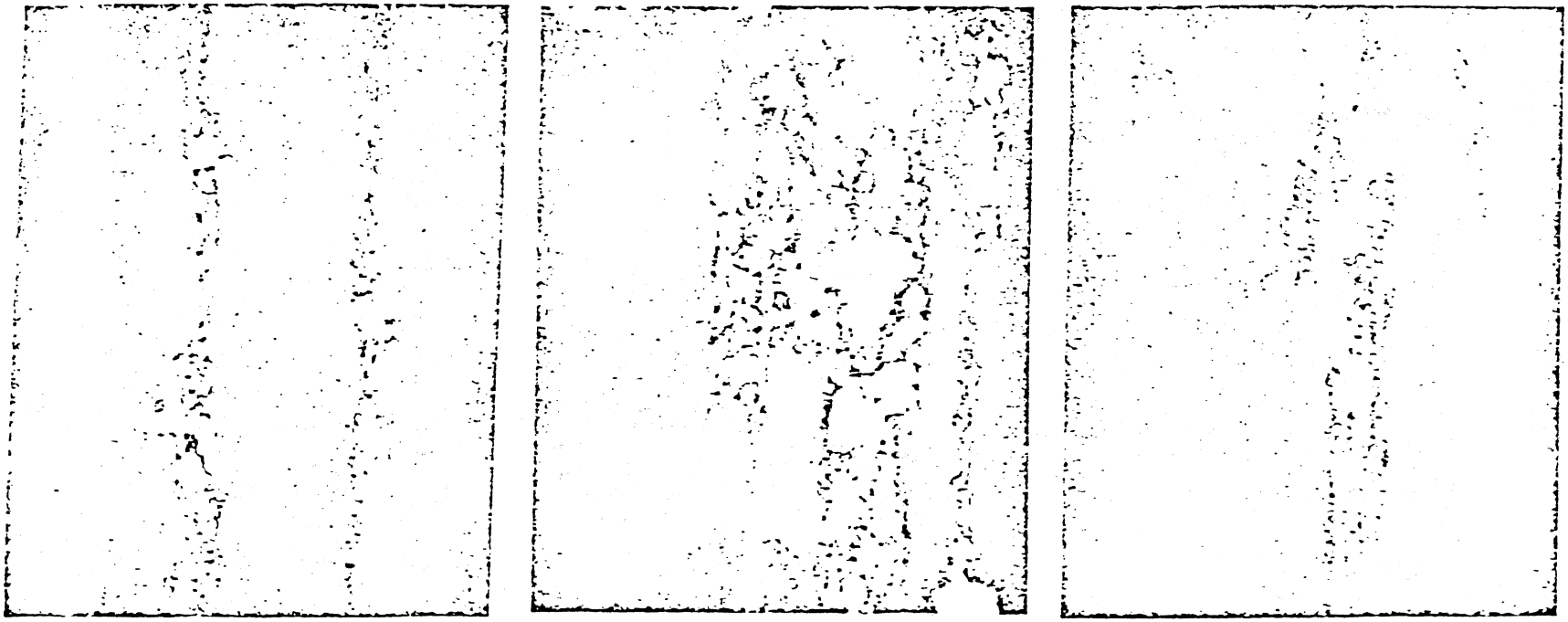

(a) 0-5 μm (b) 0-30 μm (c) 0-80 μm

Figure 38. Ferrograms of Wear Debris (54mm) From Sliding Mechanism After Exposure to 5 mg/l of Contaminant (magnification = 1000X), Wedge Condition.

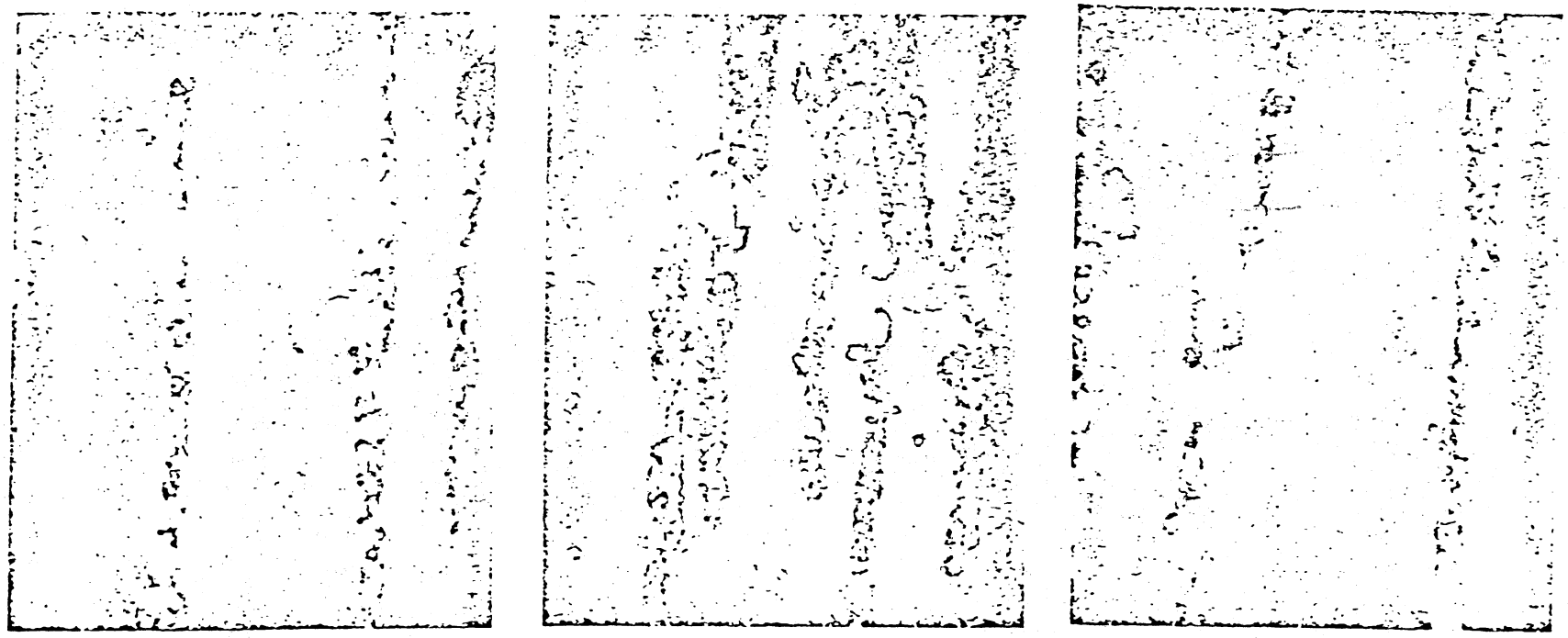

(a) 0-5 µm (b) 0-30 µm (c) 0-80 µm

Figure 39. Ferrograms of Wear Debris (54mm) From Sliding Mechanism After Exposure to 10 mg/l of Contaminant (magnification = 1000X), Wedge Condition.

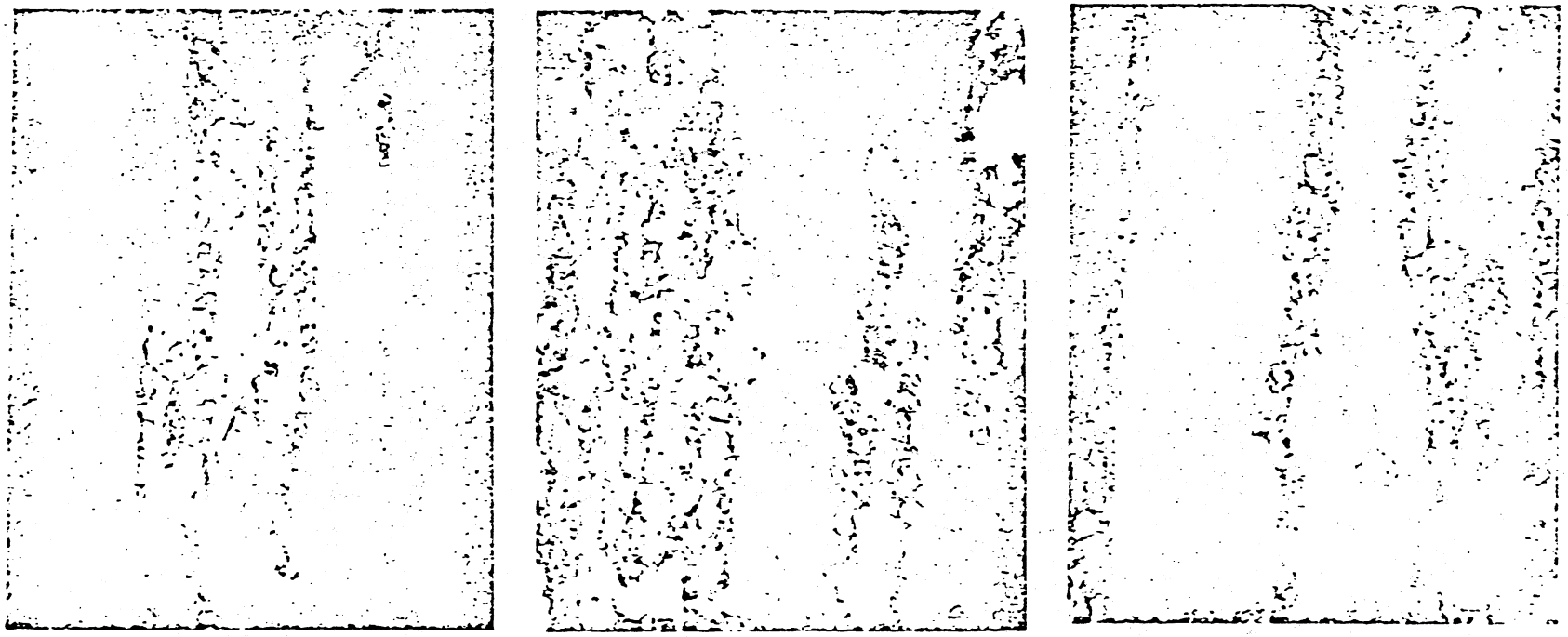

(a) 0-5 μm (b) 0-30 μm (c) 0-80 μm

Figure 40. Ferrograms of Wear Debris (54mm) From Sliding Mechanism After Exposure to 20 mg/l of Contaminant (magnification = 1000X), Wedge Condition.

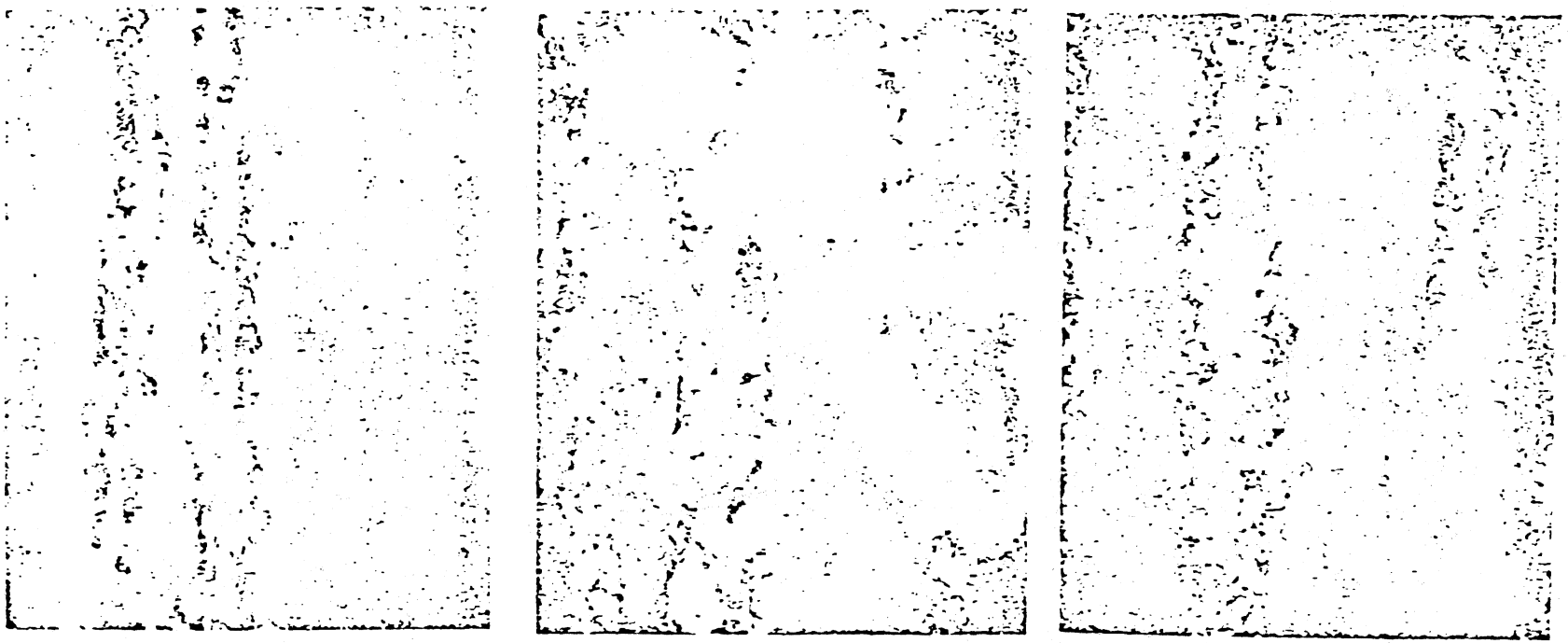

(a) 0-5 µm (b) 0-30 µm (c) 0-80 µm

Figure 41. Ferrograms of Wear Debris (54mm) From Sliding Mechanism After Exposure to 40 mg/l of Contaminant (magnification = 1000X), Wedge Condition.

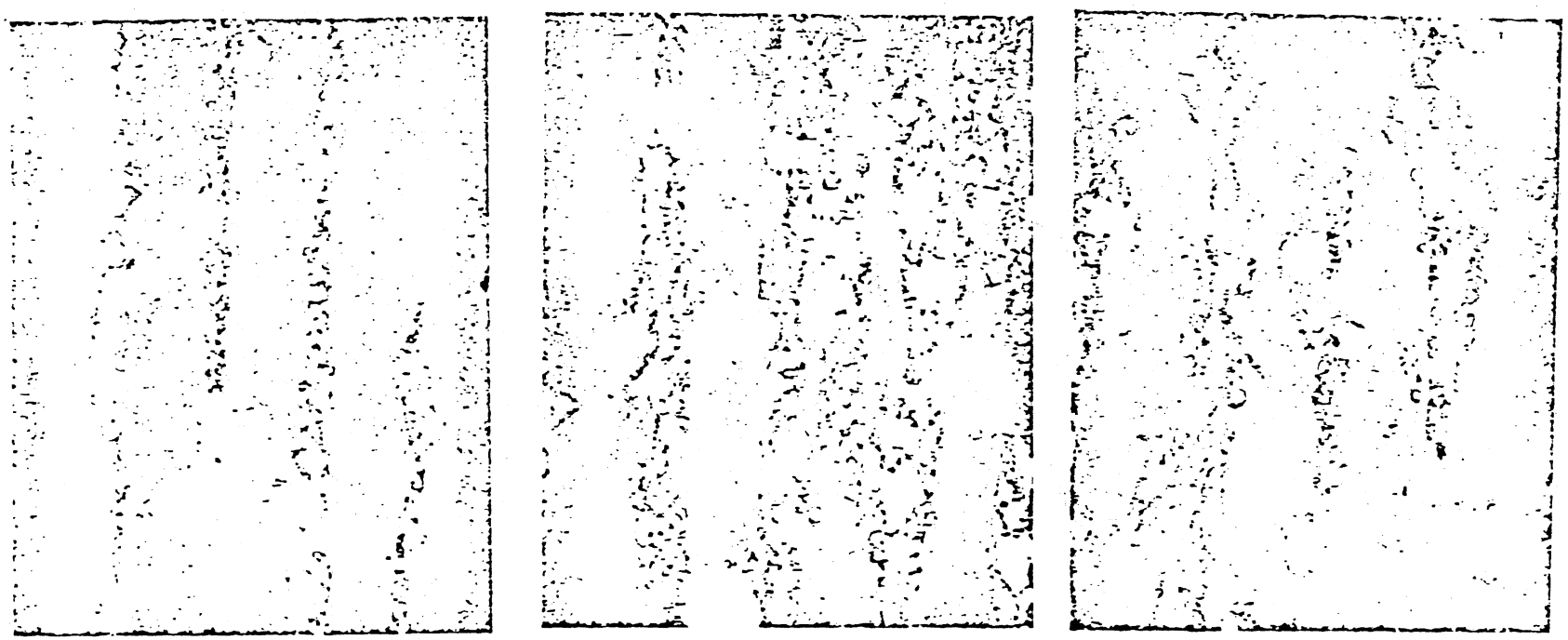

(a) 0-5 μm (b) 0-30 μm (c) 0-80 μm

Figure 42. Ferrograms of Wear Debris (54mm) From Sliding Mechanism After Exposure to 80 mg/l of Contaminant (magnification = 1000X), Wedge Condition.

VITA[2]

Ing-Tsann Hong

Candidate for the Degree of

Master of Science

Thesis: SLIDING CONTACT WEAR CAUSED BY LOOSE ABRASIVE PARTICLES IN INTERFACING LUBRICANT

Major Field: Mechanical Engineering

Biographical:

Personal Data: Born in Taichung, Taiwan, March 7, 1952, the son of Mr. and Mrs. Y. S. Hong; married in Taiwan, July 19, 1980, to Li-Jane Lin.

Education: Graduated from Taichung First High School, Taichung, Taiwan, in June, 1970; received the Bachelor of Science degree from National Central University in 1974 with a major in Physics; completed requirements for the Master of Science degree at Oklahoma State University in December, 1980.

Professional Experience: Mechanical Engineer, Kung Hwa Arsenal, 1974-1976; Mechanical Quality Control Supervisor, TIMEX Watch Company Taiwan Branch, 1976-1977; Research Assistant, Chung-Shan Institute of Science and Technology, 1977-1979; Research Associate, Fluid Power Research Center, 1979-present.

Professional and Academic Affiliations: American Society of Mechanical Engineers.